Copyright Warning & Restrictions

The copyright law of the United States (Title 17, United States Code) governs the making of photocopies or other reproductions of copyrighted material.

Under certain conditions specified in the law, libraries and archives are authorized to furnish a photocopy or other reproduction. One of these specified conditions is that the photocopy or reproduction is not to be "used for any purpose other than private study, scholarship, or research." If a, user makes a request for, or later uses, a photocopy or reproduction for purposes in excess of "fair use" that user may be liable for copyright infringement,

This institution reserves the right to refuse to accept a copying order if, in its judgment, fulfillment of the order would involve violation of copyright law.

Please Note: The author retains the copyright while the New Jersey Institute of Technology reserves the right to distribute this thesis or dissertation

Printing note: If you do not wish to print this page, then select "Pages from: first page # to: last page #" on the print dialog screen

ABSTRACT

DETERMINATION AND STUDYING OF STRESS DISTRIBUTION IN VARIOUS ANKLE-FOOT ORTHOSES: EXPERIMENTAL STRESS ANALYSIS

by
Rong Feng

Ankle-Foot Orthosis (AFO) is prescribed to constrain and inhibit abnormal motion such as "drop foot" due to stroke. Most orthoses were hand-made by orthotists according to their own experience. However, some types of AFO were easy to fatigue (out of their functional capabilities) than others due to regular usage. In order to improve the design and usage, quantitative stress analysis of different types of orthoses is needed. The objective of this project is to obtain experimental data which will confirm the results obtained from previous Finite Element Analysis (FEA)[1]. In addition, the experimental analysis is extended to obtain more data related to design parameters in various types of orthoses in order to improve the AFO design. An experimental test system and method are developed which allow accurate measurements of the strain/stress in AFOs.

Results obtained from the experimental analysis provided a clear picture of Average Peak Stress (APS) concentration and its distribution. Results further confirmed the hypothesis and results from earlier FEA[1] that peak stress in the orthosis occurs in the neck region. Thus, failure in this place is common and a better design is needed. From the present investigations, the following suggestions are made. Every AFO should be made asymmetrically and the lateral side should be wider or thicker than the medial side.

DETERMINATION AND STUDYING OF STRESS DISTRIBUTION IN VARIOUS ANKLE-FOOT ORTHOSES: EXPERIMENTAL STRESS ANALYSIS

by
Rong Feng

A Thesis
Submitted to the Faculty of
New Jersey Institute of Technology
in Partial Fulfillment of the Requirements for the Degree of
Master of Science in Biomedical Engineering

Biomedical Engineering Committee

May 1997

APPROVAL PAGE

DETERMINATION AND STUDYING OF STRESS DISTRIBUTION IN VARIOUS ANKLE-FOOT ORTHOSES: EXPERIMENTAL STRESS ANALYSIS

Rong Feng

Dr. Tina Tai-Ming Chu, Thesis Adviser — Date
Assistant Professor of Mechanical Engineering Dept., NJIT

Dr. Bernard Koplik, Committee Member — Date
Chairman and Professor of Mechanical Engineering Dept., NJIT

Dr. David Kristol, Committee Member — Date
Director and Professor of Biomedical Engineering Program, NJIT

BIOGRAPHICAL SKETCH

Author: Rong Feng

Degree: Master of Science

Date: May 1997

Undergraduate and Graduate Education:

- Master of Science in Biomedical Engineering,
  New Jersey Institute of Technology, Newark, NJ, 1997

- Bachelor of Engineering in Electrical Engineering,
  Tsinghua University, Beijing, the People's Republic of China, 1995

Major: Biomedical Engineering

Dedicated to my family

ACKNOWLEDGMENT

The author wishes to express his sincere gratitude to his thesis advisor, Dr. T. Chu, for her valuable advice and suggestions for improvement; also for her insight and constant encouragement. Special thanks are given to Dr. B. Koplik and Dr. D. Kristol for actively participating in the committee.

I also would like to express my deep appreciation to Mr. Jack Hodgins, director of Prosthetic/Orthotic Department and Mr. Gus Eppinger, orthotist, both of the Kessler Institute of Rehabilitation, for their endless resources and support.

I also would like to thank the Henry H., Kessler Foundation for supporting this research project with funding GR175. Without the financial support, this project would not have been possible.

TABLE OF CONTENTS

TABLE OF CONTENTS
(Continued)

TABLE OF CONTENTS
(Continued)

TABLE OF CONTENTS
(Continued)

LIST OF TABLES

LIST OF FIGURES

LIST OF FIGURES
(Continued)

LIST OF FIGURES
(Continued)

CHAPTER 1

INTRODUCTION

1.1 Background Information

1.1.1 Ankle-Foot Orthoses

An ankle-Foot Orthosis (AFO) [2] is a medical mechanical device to support and align the ankle and the foot, to suppress spastic and overpowering ankle and foot muscles, to assist weak and paralyzed muscles, to prevent or correct ankle and foot deformities, and to improve the functions of the ankle and foot. The specific functions of an AFO[2] are:

1. To provide mediolateral and dorsiplantar stability of the ankle during the stance phase and to keep the toes off the ground during the swing phase to prevent toe drag.
2. To improve gait by providing an additional push-off force during the later phase of the stance phase.
3. To minimize muscle imbalance at the ankle and foot by suppressing the spastic and more powerful muscles and by assisting the weak and nonfunctional muscle.
4. To protect the patient from trips and falls due to toe drag.
5. To prevent or correct abnormal ankle and foot motion due to deformities.
6. To immobilize and protect weak, inflamed, infected, painful, injured, and postsurgical lower leg.
7. To facilitate ankle and foot motion.

There are five major materials used in Ankle-Foot Orthoses[2]:

1. *Stainless steel* has been used in making uprights, ankles stirrups, foot plates, strap buckles, ankle joints, etc. It is very strong, durable, and adaptable, but it is heavy and lacks cosmetic appeal.
2. *Aluminum* is significantly weaker than stainless steel. However, it is lighter, easier to fabricate, and more cosmetically acceptable. It has been mostly used in calf bands, and in uprights brace for patients with lighter body weight.
3. *Leather* has been used in calf cuffs, and medial and lateral T-straps of the ankle.
4. *Padding materials* used include felt, plastazote, and foam rubber.
5. *Thermoplastic and thermosetting plastics* are commonly used in today's orthotic industry in fabricating molded AFO.

In today's orthotic industry such as Orthotic Prothetic Lab. Service, Inc. or Orthotic Technical Corp., two types of orthotic plastics are used: thromosetting Plastics (Thermosetts) and thermoplastics. The later including Acrylics, Polyvinyl Chloride (PVC), Polycarbonate, Polyethylene and Polypropylene. Polypropylene used in this experiment is produced by polymerization of the monomer and butadiene. Polypropylene[3] is very light, chemically inert, tough, and odorless. It has good mechanical properties and high impact strength. However, it is sensitive to extreme cold, ultraviolet light, strong oxidizing agents, and nicks and notches. Polypropylene has superb flexing properties that can withstand several million flexes before showing signs of failure. At normal temperature,

polypropylene exists above its glass-transition temperature, which makes it softer, much more flexible, and less brittle than the Acrylic. One of the major drawbacks of polypropylene is its poor shape retention. However, the high weight-strength ratio, high fatigue resistance, light weight, and excellent molding characteristics of polypropylene make it the most popular thermoplastic for all kinds of custom-made and prefabricated spinal and extremity orthoses.

1.1.2 Methods of Measuring Strain and Stress

In general, stress is the internal force per unit cross-sectional area produced by a load. There are normal stress, shear stress and stresses due to bending. Its typical unit is either PSI (pounds/in^2) or Pa (Pascal). The stresses measured in the Ankle-Foot Orthosis (AFO) in the present study are stresses due to bending. Specifically:

- Tensile stress - Force that resists being pulled apart (Fig. 1.1).
- Compressive stress - Force which resists being pushed together.

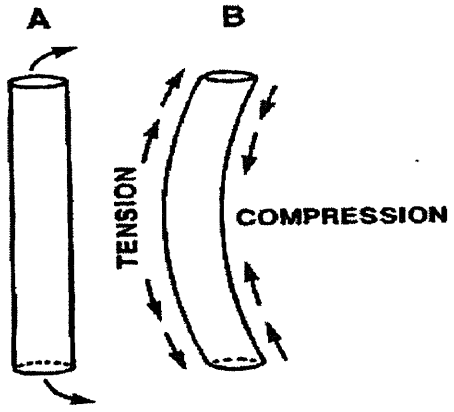

Figure 1.1 Tensile and compressive stresses due to bending.

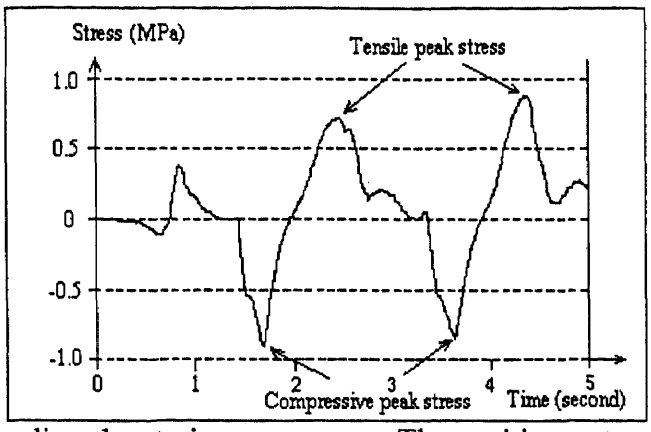

Figure 1.2 Understanding the strain gage output. The positive output is tensile strain/stress and the negative output is compressive strain/stress.

Strain is a measure of the physical deformity of a substance produced by a load acting on it. Strain can be defined as either normal strain or shear strain. The units are inch per inch or millimeter per millimeter. For each type of strain, there are two classes:

- Tensile strain due to physical elongation
- Compressive strain due to physical shortening

In general, there are four methods to measure Strain:

- Direct measurement -- Measure of dimensional changes by means of mechanical devices such as micrometers or calipers, or optical devices such as cathetometers or filar micrometers.
- Measurement using strain gages -- These transducers will convert a change in dimension (elongation or compression) into ohmic resistance which can be accurately measured by a Wheatstone bridge circuit to determine the exact magnitude of mechanical strain. It is particularly useful for measuring strains, where the use of

conventional extensometers is impracticable. The positive output is tensile strain/stress and the negative output is compressive strain/stress (Figure 1.2).

- Stress coat -- A thin layer of very brittle coating on the surface of the structure. It will crack under tension. The number of cracks per unit length and the orientation of these cracks reveal the relative amounts of tensile strain and the direction of its greatest action.
- Photoelasticity -- By applying a birefringent plastic of known physical and optical properties over the structure under study, the strain can be assessed by studying the displacement of fringes in reflected light by means of optical equipment.

1.2 Objectives

The overall objective of this project is to obtain experimental data which is intended to confirm the results obtained from previous Finite Element Analysis (FEA)[1][4]. In addition, the experimental analysis could obtain more data related to design parameters in various type of orthoses in order to improve the AFO design. A second sample with different loading force may give additional information on prediction of failure.

The specific aims of this investigation are:

1. Mount the strain gages in a manner that provides information at the different levels of strain at different locations on the AFO.
2. Develop instrumentation that could be used to simultaneously record the strains at these various locations.
3. Develop a complete experimental test procedure to collect and analyze data.

4. Conduct an extensive parameter analysis for the prediction of AFO failure.
5. Compare obtained strain information with the results from the Finite Element Analysis (FEA).

1.3 Significance

The results from experimental analysis of various types of orthoses provided a clear picture of where and how the stress is concentrated and distributed. It confirmed the hypothesis and results from earlier FEA[1][4]. That is peak stress in the orthosis occurred in the neck region, but more often in the lateral side than the medial side. The experimental results further proved that FEA is a valid method which can be used to provide quick solution to the problems such as to evaluate the AFO instead of using long-term and expensive experiment.

In today's prosthetic/orthotic industry, many orthoses fail immaturely due to partial failure, specifically at a small region such as the neck region. In addition, the obtained results indicated that not only the magnitude of the peak stress was higher on the lateral side than the medial side, it also located more often at the lateral side than the medial side. Moreover, the magnitude of stress relied on the width of the neck of the AFO. Thus, we suggest that every AFO should be made asymmetrically and the lateral side should be wider or thicker than the medial side so that the stress could evenly distribute on both sides.

From a long term view, especially from the healthcare management point of view, the patient's medical expense could be reduced as well because of this type of research.

For example, a taxi driver (major motion was dorsiflexion/planterflexion) needed an orthosis (the Standard type) after stroke. However, he complained that he damaged his orthosis every year due to constricted motion of dorsiflexion/planterflexion. From our study, we can improve the duration of usage and the reliability of performance. We suggest that his AFO should be replaced by another Standard orthosis with a wider neck especially on the lateral side. Thus, he might be able to use it for two years. On the other hand, the Standard AFO could be replaced by a Flex AFO which will provide a maximum flexibility since there was no significant change in the tensile stress and it is less than 7% in magnitude for the compressive stress during the motion of dorsiflexion/ planterflexion.

Furthermore, by increasing the lifetime of each AFO, the environment would be greatly benefited since less plastic waste will be generated.

Keywords: Strain Gage, Stress Analysis, Ankle-Foot Orthosis (AFO), Average Peak Stress (APS), Finite Element Analysis (FEA)

CHAPTER 2

LITERATURE REVIEW

Experimental stress analysis for determination of material behavior has been used for many years. However, application to medical/rehabilitation devices is a recent activity. For example, J. Kawamura *et al.*[5] biomechanically evaluated a flexible above knee system (called ISNY) using linear motion transducers and x-ray. They found that the stress changed strictly in response to the muscle activity predominant in each phase of gait. During another material evaluation, P. Convery, *et al.* [6] identified that shrinkage and distortion of polypropylene after draping does occur. In 1994, R. G. Radwin *et al.*[7] obtained biomechanical stress by repetitive manual work using frequency-weight filters instead of using a classic Wheatstone bridge circuit. However, there were no suitable analytical methods available for efficiently quantifying physical stress analysis at that time. Wong, A. K. *et al.*[7] developed a thermographic imaging system based on a 512*512 focal-plane array thermal image to perform stress analysis in 1995. However, the system was so expensive that only very few could afford it. Therefore, it is not a popular method, and generally can not be used for small-scale academic research.

In order to analyze and simulate the stress distribution of AFO by Finite Element Analysis, several investigations were conducted. In 1985, A simple 2-D Finite Element model was developed by Reddy, *et al.* [8] for computational stress analysis. However, it was not able to predict the stress change for medial-lateral variations. A 3-D Finite Element model was developed later by Chu, *et al.* [1] for a more detailed computational stress

analysis on the AFO. Although the 3-D model provided a more detailed information on static analysis, limited dynamic results were generated. Furthermore, the results need to be validated by experimental test and analysis.

In 1995, a preliminary experimental stress analysis was initiated by T. Chu and A. Gent[4][13]. Although the stress analysis was not completed due to lack of sample and equipment. A perfect bonding method for strain gage to plastic material was developed. This bonding method involved a special material surface treatment using UV light. Polypropylene is an inert material that can not be bonded/adhered to any other materials. The UV light can break the surface molecular bonding so that the other material can be bonded[11]. In our study, strain gages must be firmly bonded to the plastic surface and must be able to sustain the high stresses during jumping and running. Thus, this special surface treatment procedure is necessary.

Some research was done to compare different type of AFOs. The usage of various types of AFOs was theoretically discussed by J. E. Tomaro *et al.*[9]. Although there was no experimental data obtained to support their findings, the paper provided a theoretical basis for the use of various types of AFO in the biomechanical treatment of traumatic foot and ankle injures. A comparative study of mechanical characteristics of plastic AFOs was made by S. Yamamoto, *et al.* [10] in 1993. Using a muscle-training machine, eleven AFOs with posterior spring, anterior spring, side stay and spiral were measured. However, only dorsiflexion/plantarflexion and inversion/eversion were tested, and only the flexibility of various AFOs was compared. Clinical study of different type of AFOs to assess gait efficiency was made by D. C. Kerrigan, *et al.* [11]. Patients with gait disability reported that one or two AFOs reduced the effort necessary to walk. According to their experimental and

computational research, by comparing the energy consumption (efficiency quotient) of different AFOs, the percent change in the energy consumption with the AFOs correlated with the percent change in comfortable walking velocity.

In the present investigation, extensive experimental data was obtained which confirmed the results obtained from previous Finite Element Analysis (FEA)[1]. Ten common daily activities and patient related activities were tested on five type of AFOs. In addition, the obtained data was analyzed to compare the stress distribution due to geometry in order to improve the AFO design.

CHAPTER 3

EXPERIMENTAL METHODOLOGY

3.1 Strain Gage and Installations

3.1.1 Strain Gage Specification

The strain gage used in this experiment is called the biaxial ("Tee") rosette pattern strain gage (EA-Series, Planar rosette) manufactured by Measurements Group Inc.. It has two measuring grids perpendicular to one another (Figure 3.1) and all grids are constructed on the same plane. In this experiment, the measuring grids are vertical and horizontal grids. With two independent measurements made in perpendicular directions about a point, the principal strains can be calculated in combination as vectors. EA-series strain gages that used in this experiment have a constant foil and a tough, flexible backing. It is primarily intended for general-purpose of static and dynamic stress analysis. Table 3.1 gives brief descriptions of the EA-series strain gages.

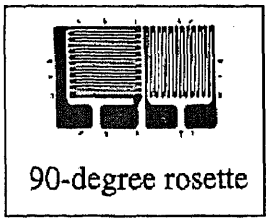

Figure 3.1 Biaxial rosette strain gage

Table 3.1 Specification of EA-Series biaxial rosette strain gage

Gage Series	Temperature Range	Strain Range	Fatigue Life Strain level/No. of Cycles
EA	Normal: -100° to 350°F	±5% for over 1/8 in	$\pm 1500/10^6$

A strain gage is an extremely sensitive device. It is capable of registering the smallest effects of an imperfect bond. Therefore, considerable attention to detail has been taken to assure stable and creep-free installations. The following procedures have been proven successful for making consistent strain gage installations.

3.1.2 Surface Preparation for Strain Gage Bonding

The surface was abraded to remove any loosely bonded adherents (scale, rust, coating, oxides, etc.), and to develop a surface texture suitable for bonding. For rough or coarse surfaces, it is necessary to start with silicon-carbide paper (SCP) of an appropriate grit. In the present experiment, a 320-grit silicon-carbide paper was used. The surface was wiped dry with the 320-grit SCP until a bright surface was produced. A sufficiently large area was cleaned to ensure that contaminants would not be dragged back into the gaging area during the step to follow.

The desired location or the test surface where the strain gage was going to be mounted was marked with a pair of crossed, perpendicular reference lines. The layout lines were burnished rather than scored or scribed. A medium-hard drafting pencil was desired. However, nothing can be bonded to the surface without a special surface treatment because the Polypropylene has an inert material property (Chu, 1996). Thus, after the layout lines were marked, the marked area was placed under UV light as closer as possible for around 30 minutes[13]. The UV light was used to break the surface molecular bound. As the final step for surface preparation, acetone, a surface cleaning agent, was used repeatedly to wash the surface thoroughly. Next, the surface was

scrubbed with cotton-tipped applicators until the clean tip used is no longer discolored when scrubbing.

3.1.3 Strain Gage Installations with Super Glue

For an instant bonding adhesive, super glue (crazy glue) was used since it was found to be the best choice among M-Bond 200 and AE-10 Adhesives. The strain gage was removed from its acetate envelop by grasping the edge with tweezers, and placed it on a cleaned glass plate with the bonding side of the gage down. A 4-to-6-inch length cellophane tape was used and anchored one end of the tape to the glass plate behind the gage. The tape was wiped firmly down over the gage using one thumb. The gage was picked up by lifting the tape at a shallow angle (30 to 45 degree) until the tape came free of the glass plate with the gage attached.

A drop of crazy glue was gently applied onto the surface in the marked area. One end of the tape was attached to the specimen (AFO) at a shallow angle. The loose end of the tape was tracked under the press to the surface so that the gage lay flat with the bonding side exposed without air bulbs under it. The tape was slightly held and slowly made a single wiping stroke over the gage/tape assembly with the thumb. Firm thumb pressure was applied to the gage area. This pressure was held for at least one minute. Wait several minutes, then the tape was removed by peeling it slowly and steadily off the surface. Terminals strips were bonded to the surface in the same way.

The above procedures result in strong mechanical bonding and overcome the presence of air bulbs and the mechanical drift problem.

3.1.4 Surface Terminals and Leadwires Soldering

Of those steps necessary for a successful gage installation, soldering leadwires to strain gages usually requires the most practice for the technician to become skilled. Moreover, of the faults in gage soldering, lifted or dislodged solder tabs are perhaps the most common. This unwelcome event is always frustrating because, when it occurs, the affected gage must be removed and replaced.

Why does this occur, and how can it be prevented? Here are the most common causes of lifted soldering tabs and the remedies for preventing them from occurring in installations.

To minimize damage to strain gages due to soldering heat, Micro-Measurements strain gages have set the gage temperatures to be +500°F (+260°C) or lower. However, for the lowest temperature solder, the temperature of the soldering iron tip typically ranged from +600°F (+315°C) to +700°F (+370°C). The lead-tin eutectic solders we used melted at +361°F (+183°C). The tip temperatures of other types of solder are even higher. It means that the dwell time of soldering iron tip on solder tabs must be limited to one or two seconds in order to reduce gage heating. The following steps should help to accomplish the soldering operation:

1 Make certain that the gage tabs are not coated with tape mastic or bonding adhesive. If necessary, clean the tabs with a soft "pink" pencil eraser. (Be certain to avoid the coarse ink erasers which will damage the tabs.)

2 Properly tin the soldering iron tip. A pool of molten solder on the tip is essential for rapid heat transfer.

3 Ensure that adequate amounts of solder flux are present. Wetting of the solder tab requires flux. Use either solder with a flux core or apply an external flux to assure the quality.

Wire Size is also a considerable concern. Wires that are too large place excessive stress on the solder tab/gage interface. When soldering EA-Series strain gages with 3-mm or larger gage lengths, it would be better to use 30- to 36-AWG single-conductor copper wire between the solder tab and the terminal strip.

3.1.5 Finishing of Strain Gage Installation

Failures of perfect bonding between the measuring surface and the strain gage can occur at the solder tab from an excessive movement of the wires after attachment. Securing the leadwire cable to test specimen and the incorporation of a strain-relief loop in the leadwires between the gage tabs and point of attachment will help to ensure that the movement of the wires at the gage tabs or terminals to be minimum.

Preattached leadwires can eliminate the need for soldering to the gage or terminal altogether in many applications. With the proper strain gage accessories and installation techniques, lifted soldering tabs can be virtually eliminated.

3.2 Instrumentation for Data Acquisition

3.2.1 System Overview

The hardware system includes bridge circuit in the breadboard, EXP16 amplifier board, DAS 800 data acquisition board which installed inside PC, and the key component PC.

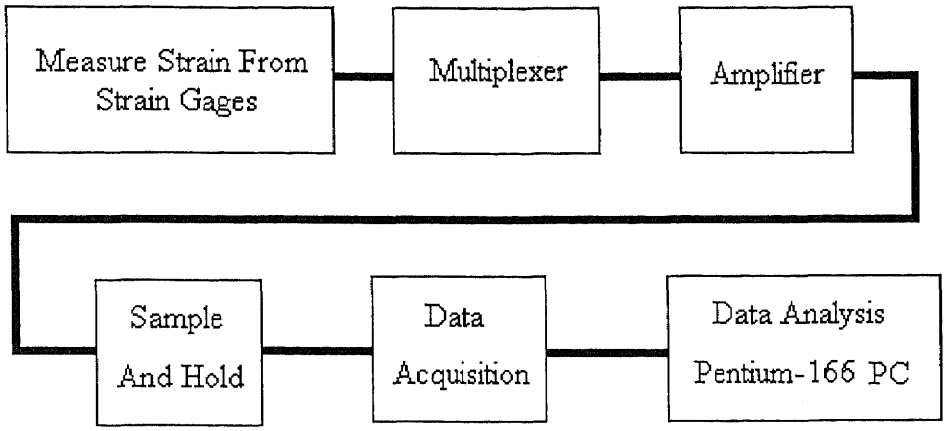

Figure 3.2 System block diagram

3.2.2 Bridge Completion

For the majority of transducer applications employing bridges, the deviation of one resistor in a bridge from an initial value must be measured as an indication of the magnitude (or a change) of the measurand. Figure 3.3 shows the bridge used in this application. R_2 is variable by ΔR, where ΔR is a deviation around zero which is a function of strain.

The relationship between the bridge output and ΔR is not linear. But for small range of ΔR it is sufficiently enough to be assumed linear for many purposes. For example, if V_{in}=5V and the maximum value of ΔR is $\pm 0.24\ \Omega$, the output of the bridge will be linear within 0.1% for a range of output from 0 to ±5mv. The sensitivity of a

bridge is the ratio of the excitation voltage (V_{in}) and the maximum expected change of the output (E_O).

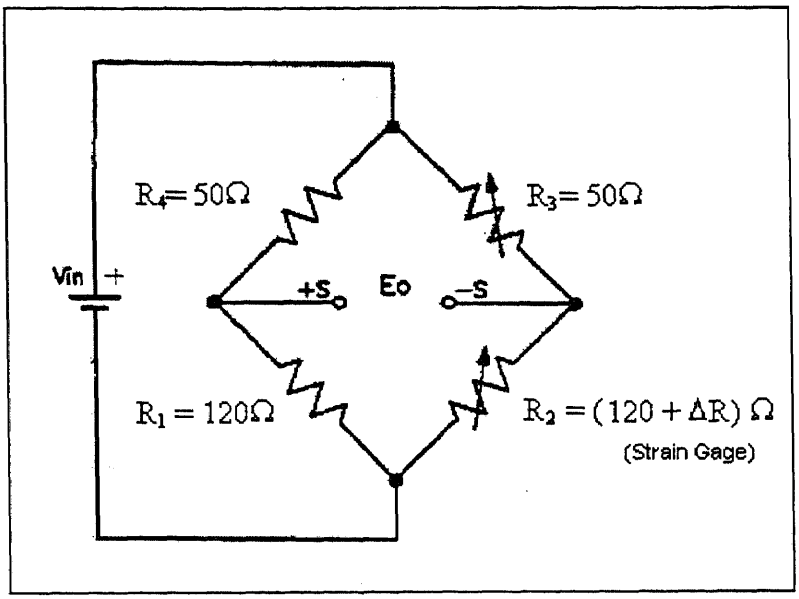

Figure 3.3 Bridge used to read deviation of a signal variable element.
V_{in}: excitation voltage, E_O: voltage change of the output, R_1 and R_4: resistors with steady value, R_3: variable resistor ranged from 0-100Ω, R_2: strain gage with approximate 120Ω initial value, ΔR: deviation which is a function of strain.

The Wheatstone bridge is used to read deviation of the signal variable element. Each strain gage has two channels: vertical and horizontal grids. Each orthosis was equipped with 8 strain gages which had totally 16 channels. In Figure 3.3, R_2 is connected to a strain gage and the initial value is approximate 120Ω. R_3 is a variable resistor initially adjusted to approximate 50Ω, the same value as R_4. V_{in} is an external power supply with 1 volt. Each strain gage has a little resistance variation. In addition, there are resistances from the wire and the cable. Thus, the initial value of R_2 is not

exactly 120Ω. In order to make the output E_O=0, each time before the testing trials, R_3 must be recalibrated and readjusted. The voltage output will be $U_A - U_B$:

$$U_A = R_1 / (R_1 + R_4) * V_{in}, \quad (3.1)$$

$$U_B = R_2 / (R_2 + R_3) * V_{in}, \quad (3.2)$$

Since $R_1 \approx R_2$, $R_3 \approx R_4$, R_3 is calibrated to make $U_A = U_B$. Thus, the output E_O is zero. When the resistance value of the strain gage has been changed (ΔR) due to the physical deformation, R_2 is changed. Thus, the voltage output:

$$E_O = R_1 / (R_2 + R_4) * U_{in} - (R_2 + \Delta R) / (R_2 + \Delta R + R_3) * V_{in}$$

$$\approx - \Delta R * V_{in} / 170 \quad (3.3)$$

The change of R_2 (which is ΔR) is very small compared with 170Ω, thus $R_1 + R_2 \approx R_3 + R_4$ = 170Ω and $E_O = - \Delta R * V_{in} / 170$. The voltage output is linear with respect to the change of the resistance of the strain gage, therefore it is linear to the strain.

3.2.3 Data Acquisition System

In this Experiment, an EXP-16 signal amplifier board and a DAS-800 data acquisition board manufactured by Keithley Instruments, Inc. were used as the interface between the analog input and the PC output.

An EXP-16 can multiplex 16 analog input signals into a single signal for amplification and input to one single-ended input channel of data acquisition system. Figure 3.4 indicates the block diagram of EXP-16. The major features of the EXP-16 board is as following:

- Expands a single-ended analog input channel of any data acquisition system into 16 differential inputs.
- Contains an instrumentation amplifier with a choice of eight switch-selectable gain settings.
- Works with Keithley MetraByte DAS-800 board.

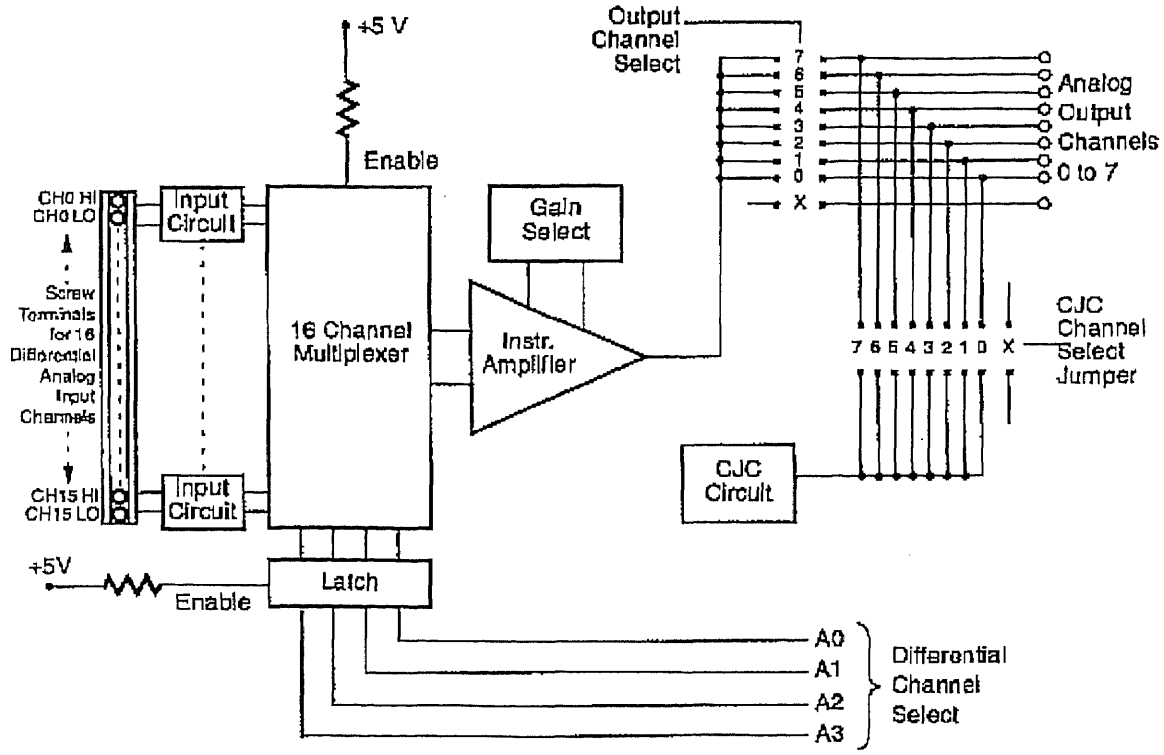

Figure 3.4 Block diagram of an EXP-16

The DAS-800 Series is a family of analog input and digital input and output (I/O) boards for an IBM® PC/XT™, AT® or compatible computer. The major features of the DAS-800 board is as following:

- Eight analog input channels (single-ended or differential).
- Fixed ±5V analog input range, software-selectable analog input ranges.

- Software-selectable conversion clock source and interrupt source.
- Three bits of digital input and four bits of digital output.

3.2.4 Wire Connection

The connectors used between each board are the D-Subminiature solder-type 25-Position males and females. Figure 3.5 indicates the output of strain gages to the corresponding location in the connectors.

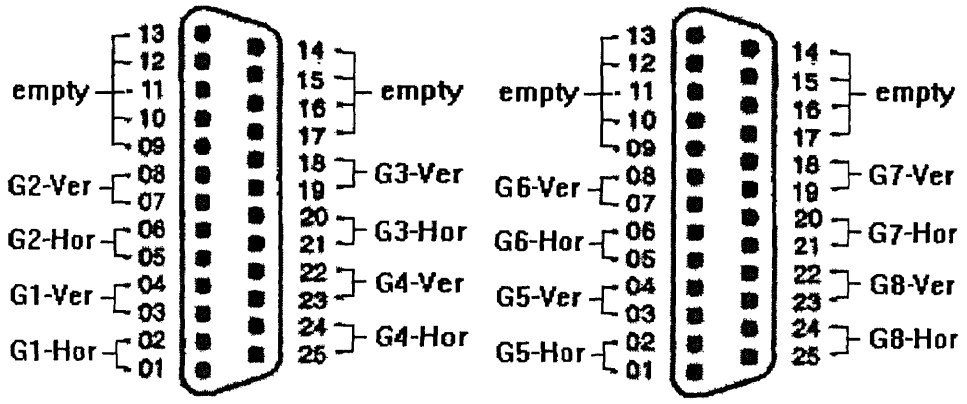

Figure 3.5 Connector settings for each channel. G1-Hor refers to the horizontal grid of strain gage 1. G1-Ver refers to the vertical grid of strain gage 1, and etc.

3.2.5 Two-Wire and Three-Wire Circuits

Static strain gage instrumentation employ some form of the Wheatstone bridge circuit to detect the resistance change in the gage due to strain.

A single active gage is connected to the Wheatstone bridge with only two wires, as shown in the accompanying schematic graph (Figure 3.6), both the wires will be in series with the gage in the same arm of the bridge circuit. One of the effects of this

arrangement is that the temperature-induced resistance changes in the leadwires are manifested as thermal output. The errors due to the leadwire resistance changes in single-gage installations with two-wire circuit can be minimized by minimizing the total leadwire resistance, that is, by using short leadwires with a largest practicable cross-section.

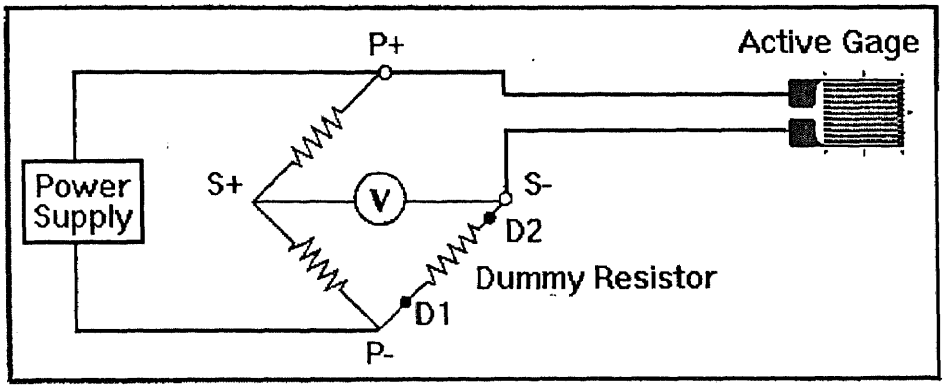

Figure 3.6 Two-wire circuit for single active gage (quarter bridge)

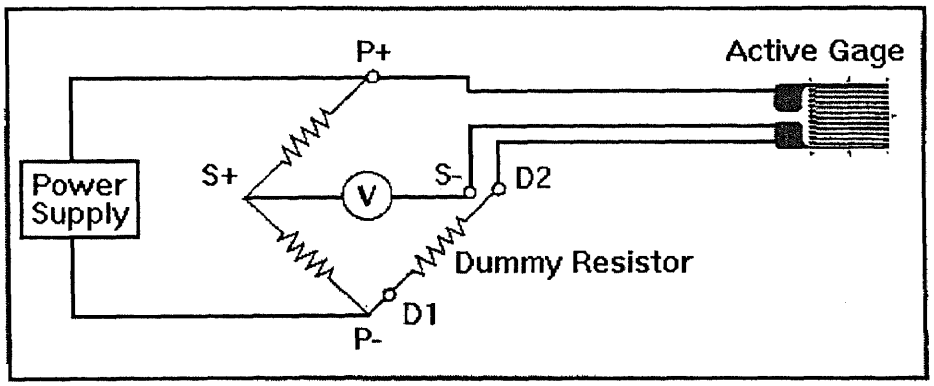

Figure 3.7 Three-wire circuit for single active gage (quarter bridge)

Leadwire effects can be virtually eliminated in single active gage installations by use the "three-wire" circuit. In this case, a third lead, representing the centerpoint connection of the bridge circuit, is brought out to one of the gage terminals (Figure 3.7).

Resistance changes in the bridge centerpoint lead do not affect bridge balance. However, under the circumstances of today's biomechanic Lab., the temperature has only a slight effect. Therefore, it can be neglected.

Contact resistance at mechanical connections within the Wheatstone bridge circuit can lead to errors in the measurement of strain. Concerning of this, the connections have been snugly made. Following bridge balance, a "wiggle" test was made on wires leading to mechanical connections. No change in balance should occur if good connections have been made.

3.3 Software Application

By using VTX™ software (producted by Keithely Metrabyte, version 1.1) with Visual Basic (version 3.0), the data obtained from data acquisition board can be displayed, analyzed and graphed.

3.3.1 Design the User Interface

The following procedures are used to design user interface to display the obtained data.

- Double-click the Microsoft Visual Basic icon in the Keithely VTX window to start Visual Basic. A new form appears.
- Move the cursor over the lower right corner of the form until the arrow changes to a double arrow, then press and hold down the left mouse button. Move the mouse to set the appropriate size of the form.

- Double-click the VTX DAS control icon in the Visual Basic Toolbox to place the control in the middle of the Visual Basic form. Move the DAS control off to the left side of the form and leave the right side space for the VTX Text control.
- Double-click the VTX Text control icon to place the control on the form. Drag the Text control to the right side of the DAS control.
- Double-click the Visual Basic command button icon three times to place the three buttons for the application on the form. Drag the buttons to the appropriate position (Figure 3-8). Save the work and ready to set the properties.

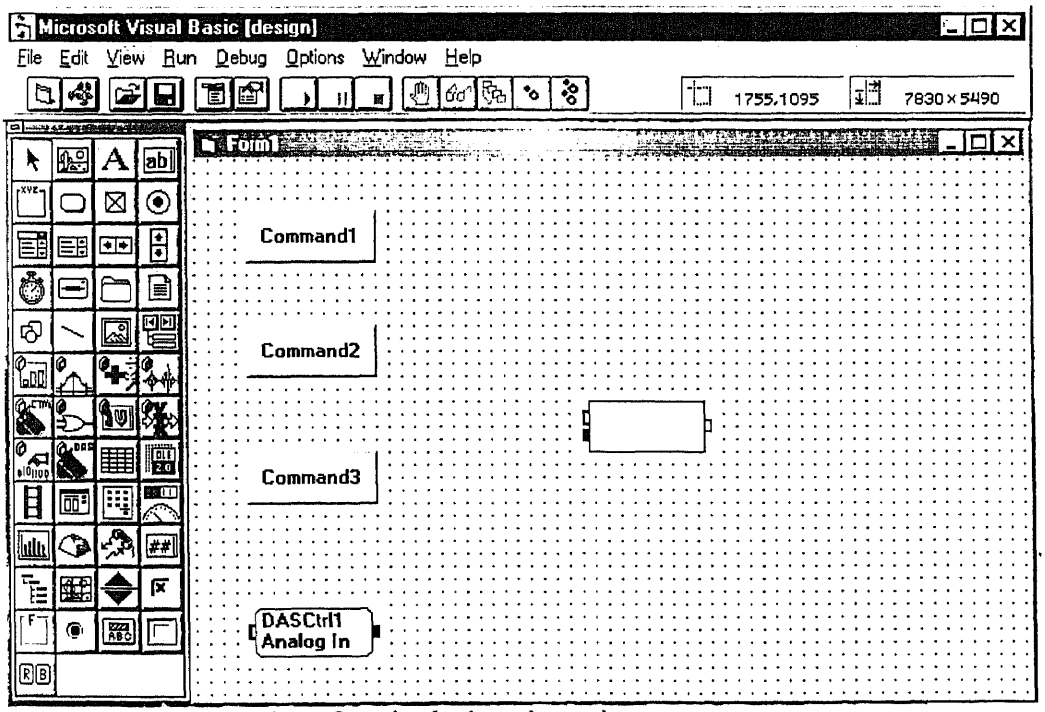

Figure 3.8 The user interface in design-time view

3.3.2 Set the Properties

1. Set the form properties: Click the form to select it and then press **F4** to display its Properties window (Figure 3.9). From the Properties window, double-click the Caption property. When the default text is highlighted, enter the following text:

   Display Analog Signal

   Locate and double-click the Name property. When the default text is highlighted, enter text: frmMain

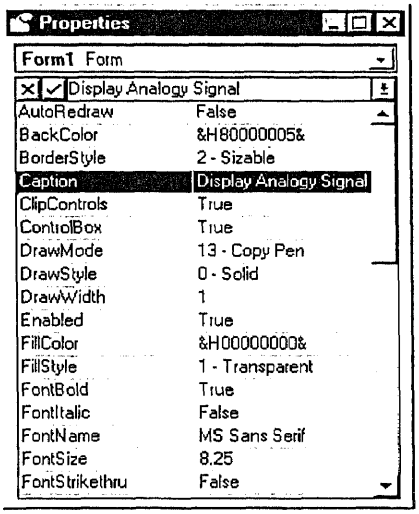

Figure 3.9 The window of properties

2. Set the DAS control properties: The DAS control properties can specify parameters for a data acquisition operation. Click the DAS control once to select it and then click the properties window to view the properties and their default settings for the DAS control. The major items to be set are:

   - Device to use for the operation (ProcessSrc property): DAS800 Board1.
   - The operation to perform (Process property): Analog In.

- When the control can start the process (ArmState property): 0 - Wait For Control Connection.
- The mode in which the operation runs (OpMode property): Interrupt.

3. Set the Graphic control properties: The Graphic control display the analog signal in graphics format. Click the Graphic control once to select it and then click the Properties windows to view the default property settings for the Graphic control. The major items to be set are:
   - The Process property setting to : Strip Chart
   - The ProcessSrc property setting to : KM_Graph
   - The Graphic control must wait until it receives the data from the DAS control before it can run the Strip Chart process. Therefore, set the default setting of ArmState property to: 0 - Wait For control connection.
4. Set the commend button properties: a commend button lets an application start, interrupt, or end a process. The button actually appears to be pushed in when clicked at run time. The steps to set the properties with the command buttons are:
   - Click the first command button (command 1) once to select it and then click the Properties windows to view the properties for a Visual Basic command button.
   - From the Properties window, double-click the caption Properties.
   - When the default text is highlighted, enter the following text: Start
   - Double-click the Name property.
   - When the default text appears in the Settings box, highlight the text and enter cmdStart

- Repeat the above steps on Commend 2 (Stop) button and commend 3 (Exit) button, enter "stop" for Stop button and "Exit" for Exit button instead of "Start" in commend 1 button. Enter "cmdStop" for Stop button and "cmdExit" for Exit button instead of "cmdstart" in commend 1 button.
- From the File menu, select Save Project.

  Now, all the properties required for the form and the controls have been set. Next, connect the VTX control to enable them to pass the analog data.

3.3.3 Connect the VTX Controls

The form now shows the commend buttons with their new captions. We will enable the DAS control to pass the analog data to the Graphic control for the display by drawing a line to wake the connection from the DAS control to the Graphic control. The control sending the data is the *source* control; the control receiving data (and/or program) is the *destination* control. Thus, the DAS control is the source control and Graphic control is the destination control. Draw the connection by performing these steps:

- Position the cursor over the right-hand side of the DAS control which is the *data output connection point*. (Figure 3.10)
- When the cursor changes to an "arrow" with a solid line, press and hold down the left mouse button.

Figure 3.10 Data output connection point

Figure 3.11 Data input connection point

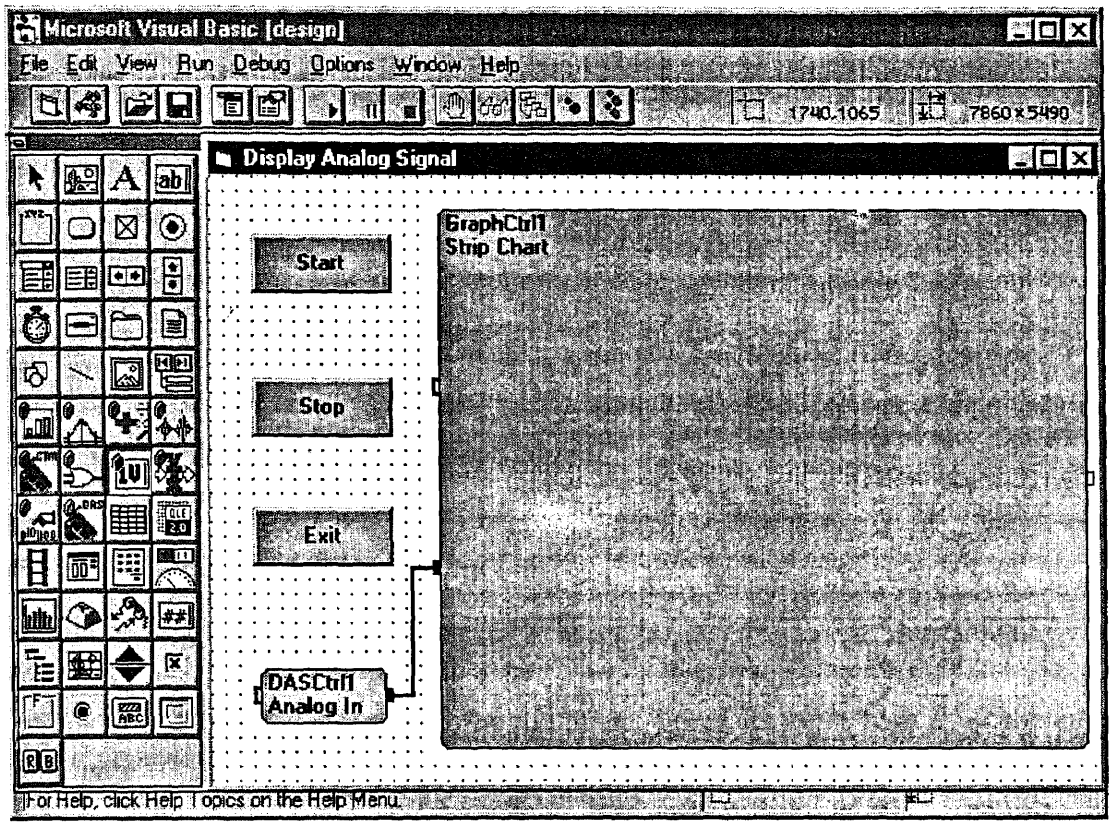

Figure 3.12 Connect graphic to VTX control

- When the arrow disappears, drag the solid line to the left-hand side of the Graphic control which is the *data input connection point.* (Figure 3.11)
- When the arrow reappears with the solid line, release the left mouse button. The connection has been made. (Figure 3.12)
- From the File menu, select Save Project.

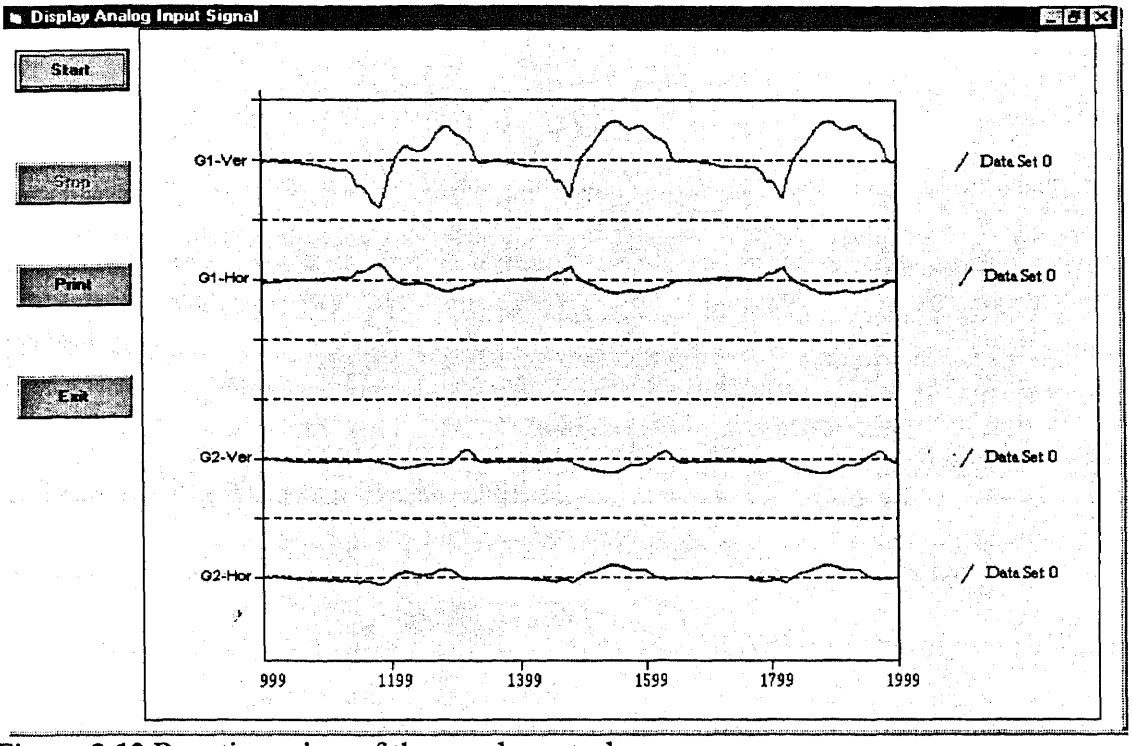

Figure 3.13 Run-time view of the graph control

3.3.4 Execute the Developed Program

1. Make sure the orthosis is connected, Bridge circuit and amplifier circuit are connected. Then select Start from the run menu. There are eight base lines should be appear in the run-time view of the Graph control (Figure 3.13). Usually, adjustment is needed for every bridge circuit to set the eight base lines display in a proper position on the screen.
2. Start to perform action (walk, jump, etc.) on the orthosis, each of the eight lines will show its curve according to the changes of strain as function of time on each strain gage.
3. To re-activate the Start button, click the Stop button.
4. Repeat steps 2 and 3 for different trials.

5. To exit the program, click the Exit button.

The application with Visual Basic and VTX software for data acquisition and graphing data from orthosis has completed. Next, quantitative data analysis were performed.

3.3.5 Transferring Data to a Spreadsheet

By using of Transfer control function in VTX, the data from DAS control can be restored to spreadsheet such as Lotus 1-2-3, Quattro Pro or Microsoft Excel. The Microsoft Excel is used as a source or destination application in this experiment. Here is the steps of transferring data from DAS control to Microsoft Excel using Transfer control function:

1. Drop the Transfer control on the form showed in Figure 3.13.
2. Set the Process property of the Transfer control to DDE to send the data to a spreadsheet file.
3. Click the ellipsis as indicated for the (More) property to display the More Properties window, then select Out From VTX for the Direction property.
4. Use the other DDE process properties to specify the spreadsheet application, spreadsheet file, and starting location in the spreadsheet for the data.
5. Connect the data output connection of the DAS control to the data input connection point of the Transfer control.
6. Save the project files and run the application. Using this software application with data acquisition system, the strain changes in AFO can be displayed accurately.

CHAPTER 4

DATA ANALYSIS AND RESULTS

4.1 Orthoses Specification and Strain Gage Location

Five types of AFOs were custom-made by Kessler Institute of Rehabilitation, New Jersey. They were fitted onto a normal subject. The five AFOs are:

1 the Flex orthosis -- used for minor injured patient. It is more comfortable, more flexible and convenient. However, it provides minimum support (Figure 4.1).

2 the Standard orthosis -- the most popular one and used for regular patient. It also provides limited support (Figure 4.1).

3 the Moderate orthosis -- wider in the neck region than the Standard one. It provides less dorsiflexion/planterflexion but more support (Figure 4.1).

4 the Solid orthosis -- wider in the neck region than the Moderate one. It prohibits dorsiflexion/planterflexion and provides much more necking support (Figure 4.1).

5 the Varus orthosis -- the widest in the neck region to prohibit dorsiflexion/ planterflexion. It has additional support part in the lateral upper-neck region to prohibit inversion and eversion. It provides the maximum support and it is used for severe injured patient (Figure 4.1).

The materials of the AFOs were Colyene™ Co-polymer, Fleshtones & Colors. More than 90% of this material is polypropylene. Thus, its mechanical property is similar to polypropylene. The anthropometric data of the five orthoses were measured and listed in Table 4.1. Eight strain gages were installed to the specific locations (Table 4.2) along

the lateral side, the medial side and the middle of the lower neck of the orthoses. Each strain gage recorded the dynamic stress change due to different motions. The Average Peak Stress (APS) at those eight selected locations was obtained. The stress analysis was able to determine the location of maximum Average Peak Stress (APS) in each orthosis. The APS distribution contour among the eight test locations provided the possibility for prediction of the failure (material-broken) area.

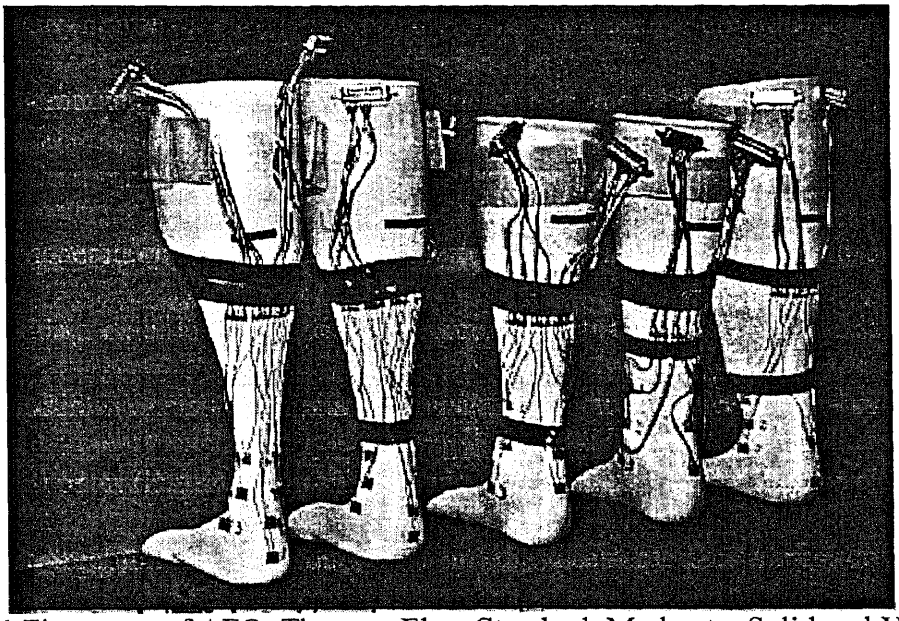

Figure 4.1 Five types of AFO. They are Flex, Standard, Moderate, Solid and Varus AFO from the left to the right.

Table 4.1 The anthropometric data of the orthoses (refer to Figure 4.2).

Orthosis Type	Varus	Solid	Moderate	Standard	Flex
Symmetric? (Y/N)	N	N	N	N	N
Width of Neck (cm)	11.8	11.8	9.9	7.6	4.9
Height (cm)	41.0	36.5	37.0	39.5	40.0

Length (cm)	17.0-17.5
Thickness(cm)	0.39-0.41

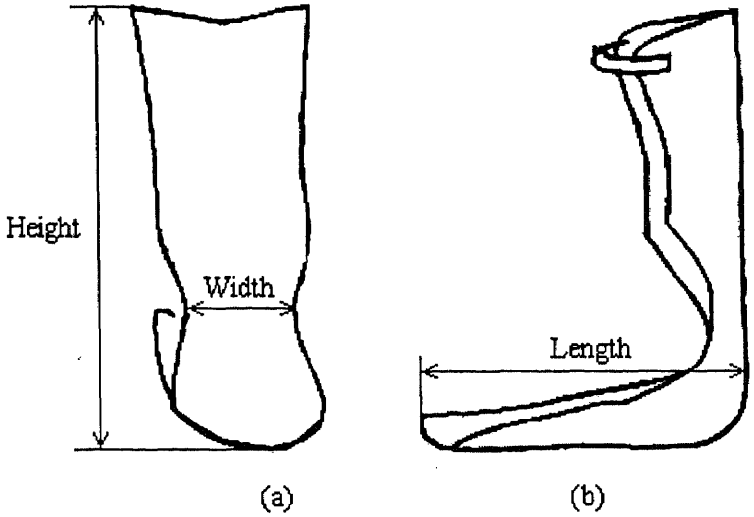

Figure 4.2 The anthropometric representation of the ankle-foot orthosis.

Table 4.2 Strain gage series number and their location (refer to Figure 4.3).

Strain Gage No.	Strain Gage Location	
G1	lateral side	upper-neck
G2	lateral side	neck
G3	lateral side	lower-neck
G4	middle	neck
G5	middle	lower-neck
G6	medial side	upper-neck
G7	medial side	lower-neck
G8	medial side	upper-heel

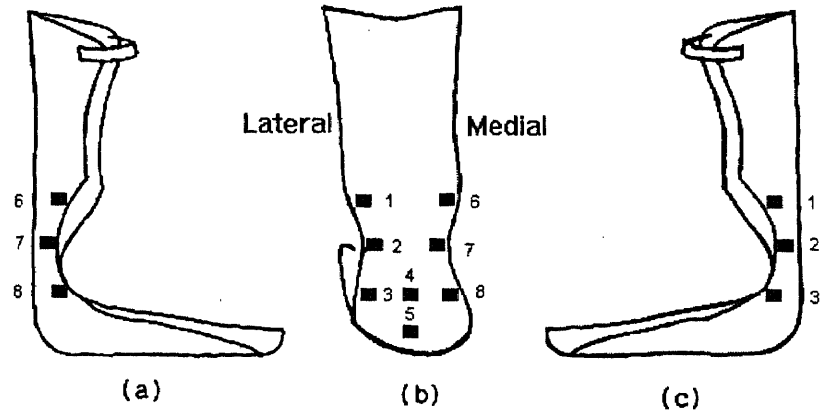

Figure 4.3 Schematic representation of the sample AFO with strain gages.
(A) view from the left (medial); (b) view from the back; (c) view from the right (lateral)

In the present experiment, the neck of the AFOs refers to the narrowest place of the back of the orthosis, where gage 2 and gage 7 (Figure 4.3) were located. Upper-neck and lower-neck refer to 2-3 cm above or below the neck. Gage 1 and gage 6 were located at the upper-neck. Gage 3 and gage 8 were located at the lower-neck. Gage 4 and gage 5 were located at the middle of the back of the orthosis from lower-neck to heel region.

4.2 Test Conditions

Motions (totally ten) of the stance phase and the swing phase were two test conditions in this experiment. In each phase, each chosen movement was tested for three trials. Each trial was recorded at normal conditions. That is, the patient always walked at almost the same speed and jumped at almost the same height when wearing the different orthoses in order to make the results comparable. The resultant stress was calculated from the vertical and horizontal components. The majority came from the vertical component.

4.2.1 Motions Involved in the Stance Phase of a Gait

Four walking motions (slow forward walk, fast forward walk, running, backward walk) and three in position motions (jumping, standing up/sitting down, lifting object) were selected to be tested in the stance phase. There motions are general or common motions need to perform during daily activities.

At any time during a motion, the 16 channels recorded either positive or negative value. The positive values represent the tensile stress magnitude and the negative values represent the compressive stress magnitude.

4.2.1.1 Slow Forward Walk: The motion of slowly walk forward is the most common human movement in nature. Slow walk usually occurred for the older, or disabled patient who needs some type of support, or the patient who is in the recovery process.

Heel strike or toe-off produced both tensile and compressive stresses at different locations. However, the highest magnitude stress generated during heel strike was compressive peak stress. The highest magnitude stress generated during toe-off was tensile peak stress. The maximum compressive peak stress occurred during the heel strike and the maximum tensile peak stress occurred during the toe-off. G2 (refers to strain gage 2) indicated both stresses (Figure 4.4). Thus, the compressive APS distribution profile obtained from all 8 gages in each orthosis revealed the peak stress concentration during the heel strike. The tensile APS distribution profile revealed the peak stress concentration during toe-off.

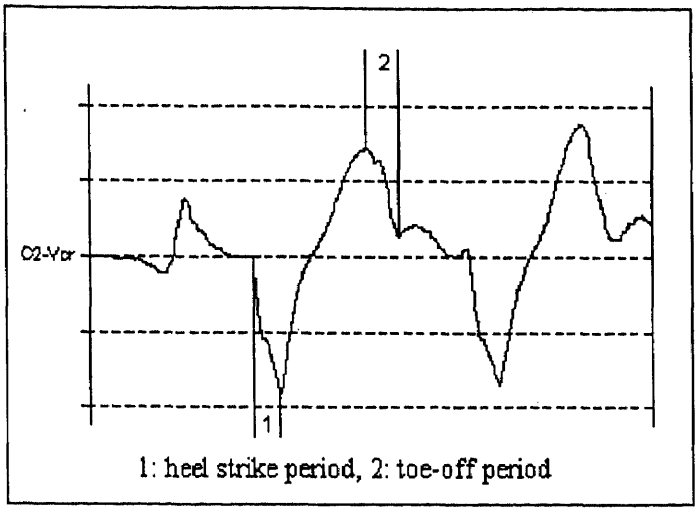

Figure 4.4 Labels 1 and 2 indicate two stages of the stance phase of the gait in slow forward walk with the Flex orthosis

The maximum tensile APS of the Varus orthosis (0.35 MPa) occurred at G2 and G1 (Figure 4.5). However, compared with the Standard and the Flex orthoses, this magnitude was less than half. The highest tensile APS for the Solid (0.39MPa) and the Moderate orthoses (0.74MPa) occur at G6 and G1, the upper-neck of both sides. For the standard orthosis, it was found that the tensile APS was located at G2 and G1, then followed by G8, G3 and G4. For the Flex orthosis, the tensile APS was located at G2, followed by G6 and G3. The distribution clearly showed a shear failure. The tensile peak stresses of the Varus, the Standard and the Flex orthoses were all concentrated in the neck region of the lateral side.

In a similar fashion as the tensile APS, most compressive APS occurred at the identical place but at different period such as the heel strike. However, with the Varus and the Standard AFO, the tensile APS at neck is higher at the upper neck than the lower neck

(refer to the direction of the arrows), the compressive APS at lower neck is higher than at the upper neck (Figure 4.6).

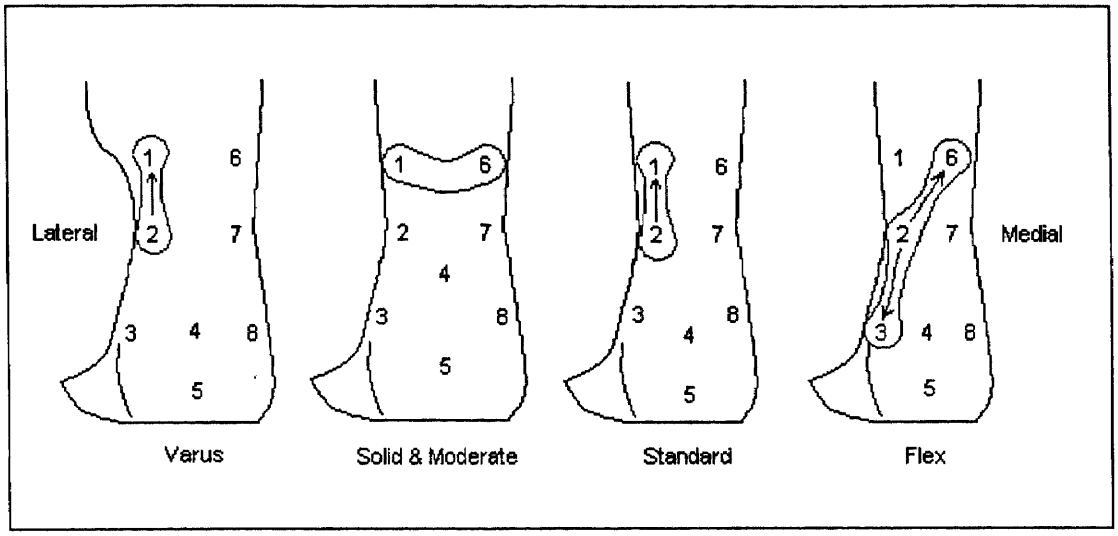

Figure 4.5 Tensile APS (toe-off) distribution profile in slow forward walk. Circled region shows the high APS concentration. Arrow indicates the change of the magnitude of APS from high to low. If no arrow indication, stresses are similar.

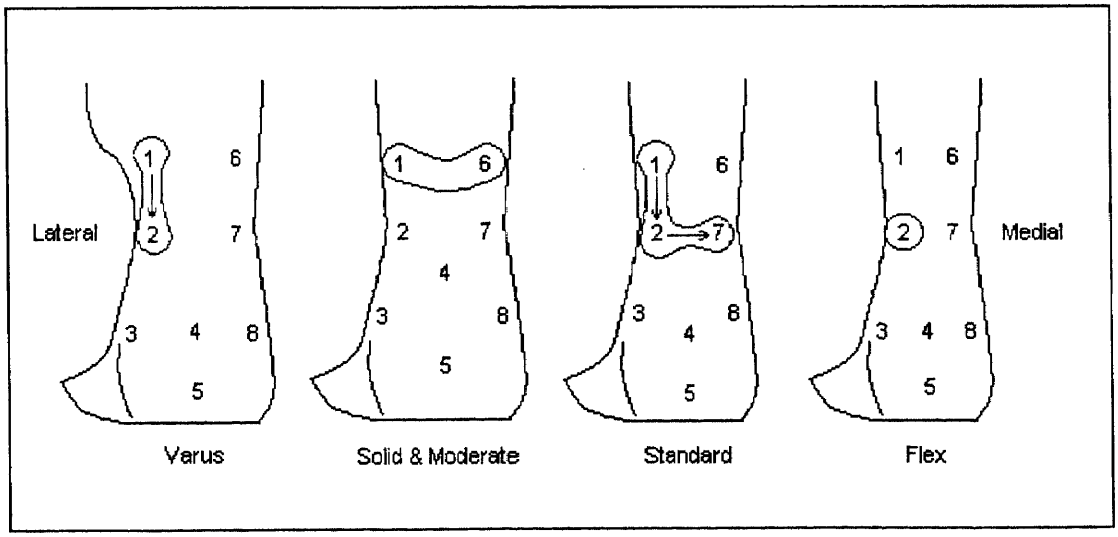

Figure 4.6 Compressive APS (heel strike) distribution profile in slow forward walk. Circled region shows the high APS concentration. Arrow indicates the change of the magnitude of APS from high to low. If no arrow indication, stresses are similar.

Table 4.3 Magnitude and location of maximum peak stress for slow forward walk

Orthosis Type	Magnitude & Location of Peak Stress	
	Tensile Peak Stress (0.1*MPa)	Compressive Peak Stress (0.1*MPa)
Varus	3.5 @ upper-neck, lateral side	5.0 @ upper-neck, lateral side
Solid	3.9 @ upper-neck, both sides	4.9 @ upper-neck, both side
Moderate	7.4 @ upper-neck, both side	5.5 @ upper-neck, both side
Standard	8.4 @ upper-neck, lateral side	6.0 @ upper-neck, lateral side
Flex	9.0 @ neck, lateral side	9.0 @ neck, lateral side

Note: refer to Figure 4.5 and Figure 4.6 for detail.

4.2.1.2 Fast Forward Walk: During the fast forward walk, the tensile APS concentration of the Varus and the Standard orthoses occurred at G1 and G2 (Figure 4.7), For the Flex orthosis, the tensile APS occurred at G2. It is the same as in slow walk. For the Solid and the Moderate orthoses, the tensile APS was concentrated at G6, followed by G1, G2, G3 (the lateral upper-neck) which had almost the same intensity.

For the Varus and the Flex orthoses, the compressive APS (during heel strike) was located at exact the same place as the tensile APS (during toe-off). However, for the other three type of orthoses, it showed the differences. The compressive peak stresses in the Solid and the Moderate orthoses were concentrated not only at G1 and G6, but also at G3 and G8 (the lower neck of both side) (Figure 4.8). For the Standard orthosis, the highest two peak stresses were found at G1 and G2. However, the compressive stresses at G3 (lower-neck of lateral side) and G7 were almost the same as that at G2.

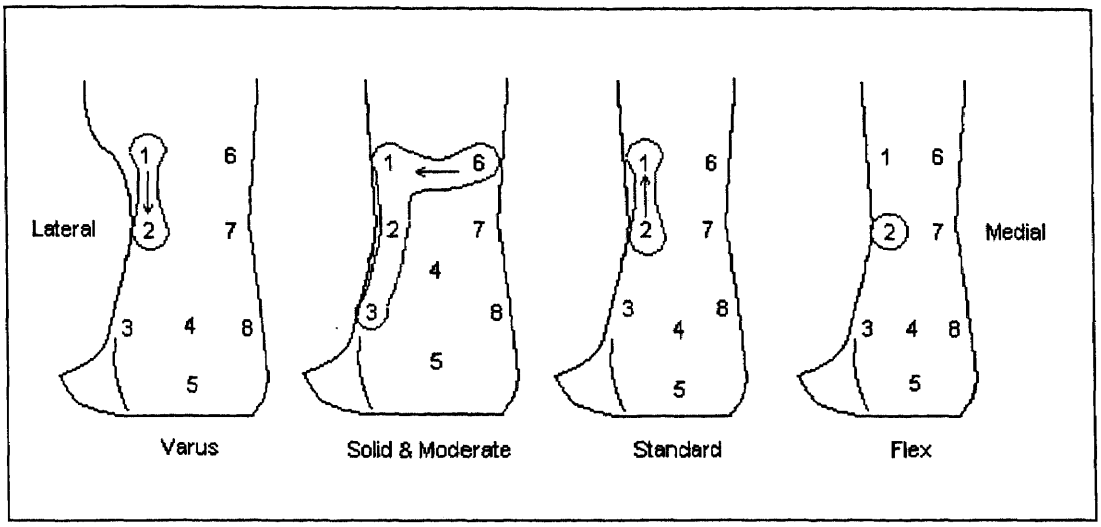

Figure 4.7 Tensile APS (toe-off) distribution profile in fast forward walk. Circled region shows the high APS concentration. Arrow indicates the change of the magnitude of APS from high to low. If no arrow indication, stresses are similar.

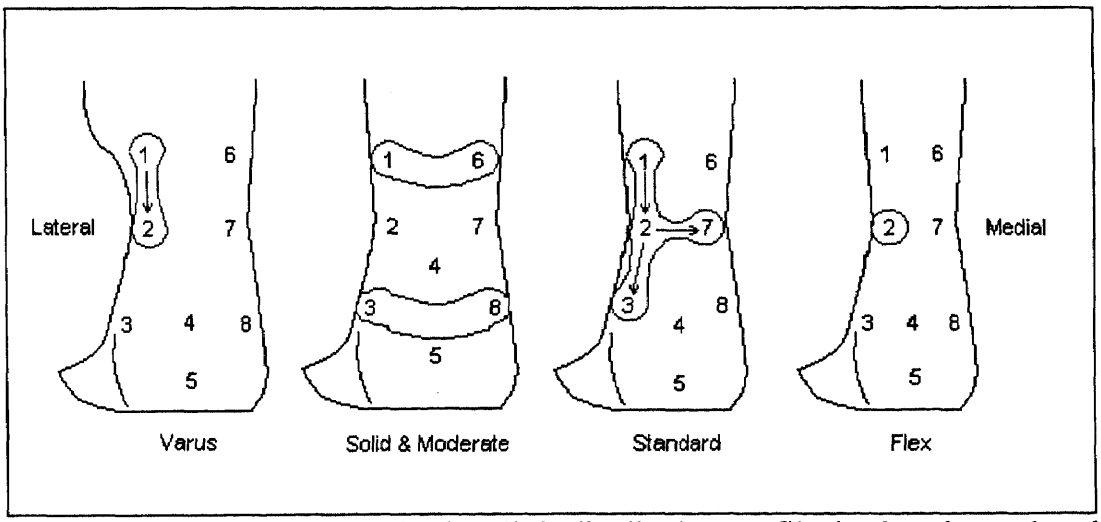

Figure 4.8 Compressive APS (heel strike) distribution profile in fast forward walk. Circled region shows the high APS concentration. Arrow indicates the change of the magnitude of APS from high to low. If no arrow indication, stresses are similar.

Table 4.4 Magnitude and location of maximum peak stress for fast forward walk

Orthosis Type	Magnitude & Location of Peak Stress	
	Tensile Peak Stress (0.1*MPa)	Compressive Peak Stress (0.1*MPa)
Varus	3.4 @ upper-neck, lateral side	5.0 @ upper-neck, lateral side

Solid	5.5 @ upper-neck, lateral side	4.8 @ upper & lower-neck, both side
Moderate	6.9 @ upper-neck, both side	6.1 @ upper & lower-neck, both side
Standard	7.0 @ upper-neck, lateral side	7.0 @ all neck, lateral side
Flex	8.5 @ neck, lateral side	7.0 @ neck, lateral side

Note: refer to Figure 4.7 and Figure 4.8 for detail.

4.2.1.3 Running: The tensile APS concentration of the Varus and the Flex orthoses occurred at G2 (Figure 4.9). For the Standard orthosis, the tensile APS occurred at G1 and G2, which was the same as in slow walk. For the Solid and the Moderate orthoses, the tensile APS was showed in two concentrated areas: one was at G1 and G6, the other was at G4 and G5 (the lower-neck to heel region in middle) (Figure 4.8).

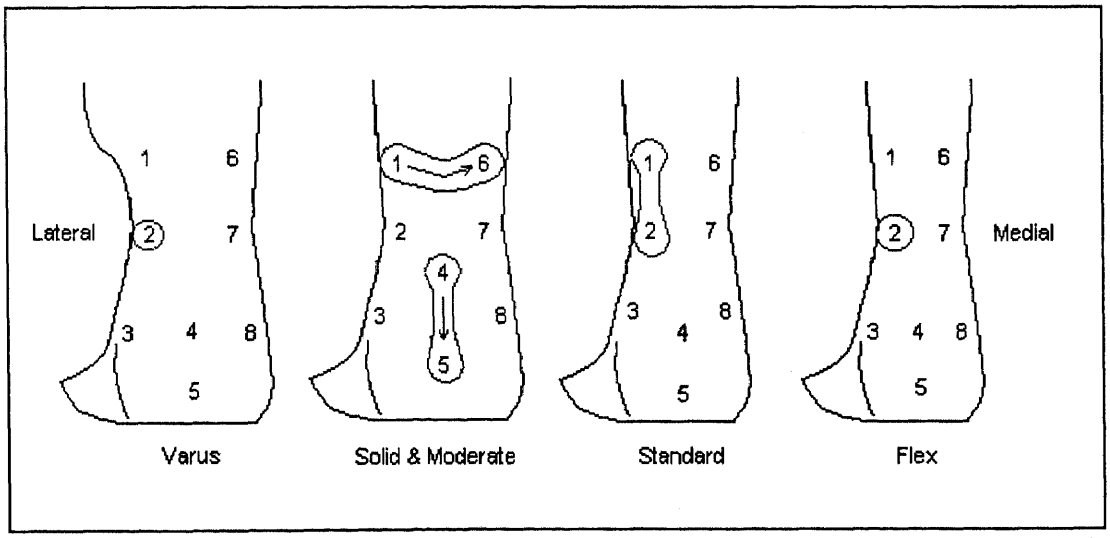

Figure 4.9 Tensile APS distribution profile in running. Circled region shows the high APS concentration. Arrow indicates the change of the magnitude of APS from high to low. If no arrow indication, stresses are similar.

The compressive APS was located at G1 for the Varus orthosis. The compressive peak stresses in the Solid and the Moderate orthoses were concentrated only at G1 and G6 (Figure 4.10). In the Standard orthosis, the highest two peak stress were found at G2. However, the magnitude of the compressive stresses at G3, G7 and G1 were all found to be close to that at G2. As for the Flex orthosis, the whole neck and upper-neck were highly concentrated. However, the magnitude of the compressive APS was the lowest one (0.34 MPa). The Moderate orthosis sustained the highest compressive APS (0.96 MPa).

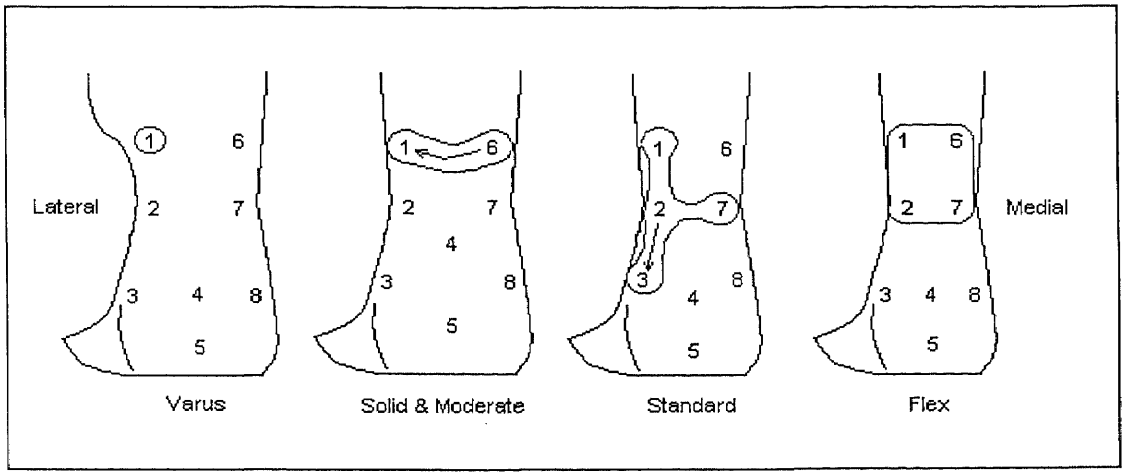

Figure 4.10 Compressive APS distribution profile in running. Circled region shows the high APS concentration. Arrow indicates the change of the magnitude of APS from high to low. If no arrow indication, stresses are similar.

Table 4.5 Magnitude and location of maximum peak stress for running

Orthosis Type	Magnitude & Location of Peak Stress	
	Tensile Peak Stress (0.1*MPa)	Compressive Peak Stress (0.1*MPa)
Varus	3.0 @ neck, lateral side	5.0 @ upper-neck, lateral side
Solid	5.5 @ upper-neck, both sides & lower-neck, middle	6.5 @ upper-neck, both side

Moderate	8.5 @ upper-neck, both sides & lower-neck, middle	9.5 @ upper-neck, both side
Standard	9.6 @ upper-neck, lateral side	6.5 @ all-neck, lateral side
Flex	16.5 @ neck, lateral side	3.4 @ neck & upper-neck, both sides

4.2.1.4 Backward Walk: A gait of walk backward begins with a toe strike, followed by foot flat and then heel strike (Figure 4.11). The tensile peak stress occurred during the toe strike and the compressive peak stress occurred during the heel strike are shown in Figure 4.12 and Figure 4.13. More specific, the tensile APS distribution profile in each orthosis revealed the stress concentration of toe strike, the compressive APS distribution profile revealed the stress concentration of heel strike. The stress curves of walk backward is the exact reverse of walk forward.

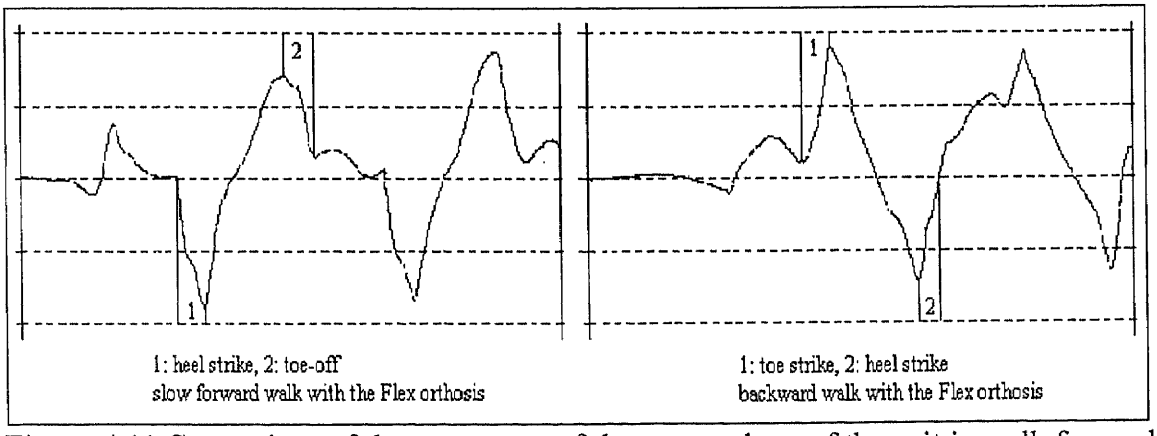

Figure 4.11 Comparison of the two stages of the stance phase of the gait in walk forward and backward with the Flex orthosis.

The tensile APS concentration of the AFOs in backward walk occurred at almost the same region as that in the forward walk. For the Varus orthosis, the tensile APS was located at G1 (Figure 4.12), With the Solid and the Moderate orthoses, it was located at G1 and G6. However, G4 also recorded a high stress. For the Standard orthosis, the tensile APS occurred at G1 and G2. For the Flex orthosis, as regular, the tensile APS was found at G2. The magnitude of tensile APS increased as the width of the orthotic neck decreased.

The compressive APS was located at G1 for the Varus orthosis. For the Solid and the Moderate orthoses. The compressive APS was concentrated at G1 and G6 (Figure 4.13). In the Standard orthosis, the highest peak stress were found at G1. However, the compressive stresses at G2 and G7 were also very high. As for the Flex orthosis, the highest compressive APS was located at G2, followed by G1 and G6. However, the highest magnitude of compressive APS was found in the Moderate orthosis (0.8 MPa).

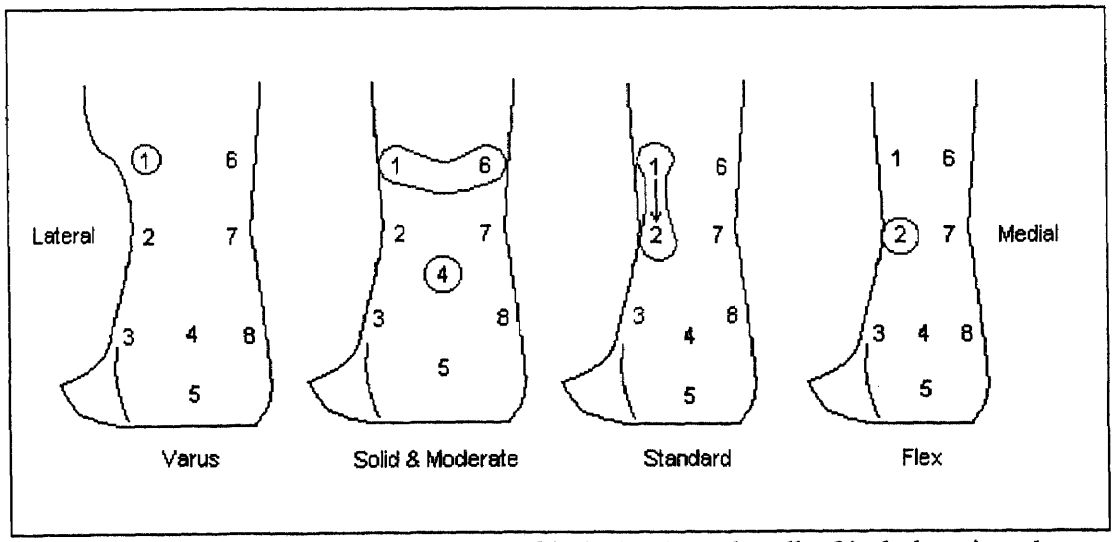

Figure 4.12 Tensile APS distribution profile in backward walk. Circled region shows the high APS concentration. Arrow indicates the change of the magnitude of APS from high to low. If no arrow indication, stresses are similar.

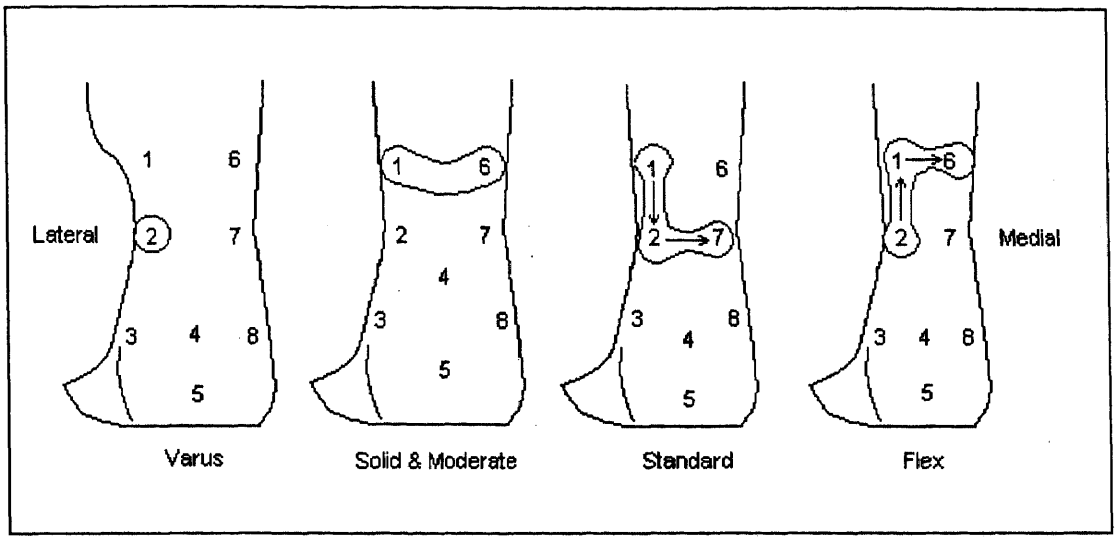

Figure 4.13 Compressive APS distribution profile in backward walk. Circled region shows the high APS concentration. Arrow indicates the change of the magnitude of APS from high to low. If no arrow indication, stresses are similar.

Table 4.6 Magnitude and location of maximum peak stress for backward walk

Orthosis Type	Magnitude & Location of Peak Stress	
	Tensile Peak Stress (0.1*MPa)	Compressive Peak Stress (0.1*MPa)
Varus	2.5 @ upper-neck, lateral side	2.5 @ neck, lateral side
Solid	4.9 @ upper-neck, both sides & lower-neck, middle	3.0 @ upper-neck, both side
Moderate	6.5 @ upper-neck, both sides & lower-neck, middle	8.0 @ upper-neck, both side
Standard	8.5 @ neck & upper-neck, lateral side	7.8 @ neck & upper-neck, lateral side
Flex	9.6 @ neck, lateral side	7.0 @ neck & upper-neck, lateral side

4.2.1.5 In Position Jumping (4 inches high): Except the increment of the stress magnitude (Table 4.7), there is no significant difference in tensile APS concentration or

distribution (Figure 4.14) compared with those in walking. However, the compressive APS concentration altered noticeably.

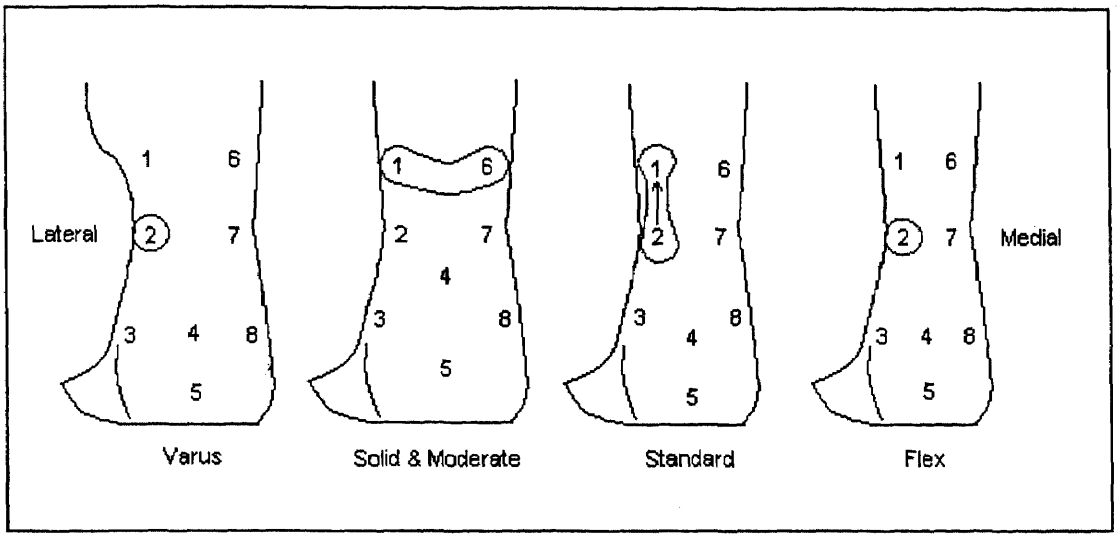

Figure 4.14 Tensile APS distribution profile in jumping. Circled region shows the high APS concentration. Arrow indicates the change of the magnitude of APS from high to low. If no arrow indication, stresses are similar.

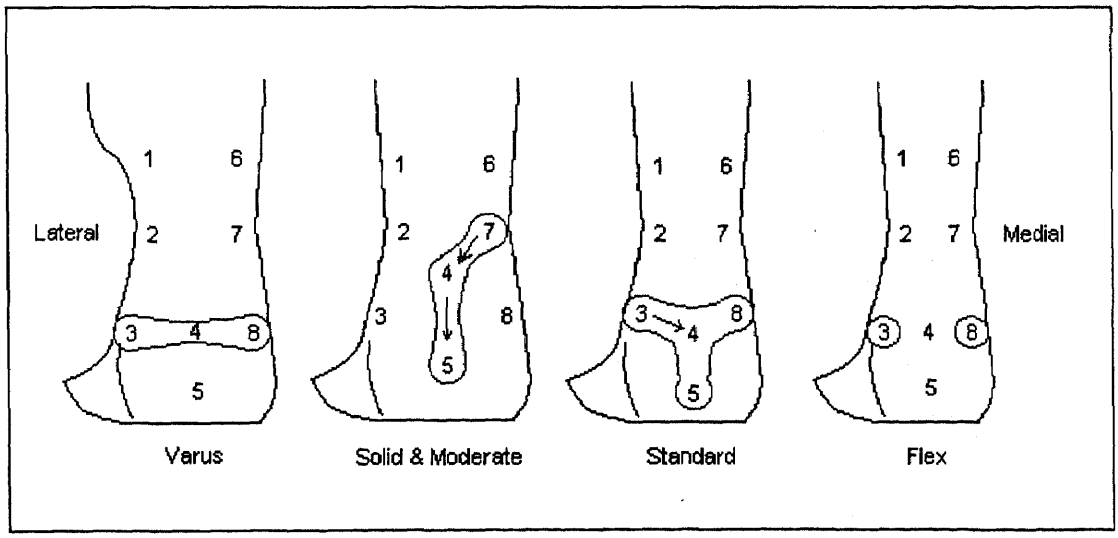

Figure 4.15 Compressive APS distribution profile in jumping. Circled region shows the high APS concentration. Arrow indicates the change of the magnitude of APS from high to low. If no arrow indication, stresses are similar.

The compressive APS concentration shifted to the lower-neck and the heel region (Figure 4.15). For the Varus orthosis, the concentration was found at G3, G4 and G8. For the Solid and the Moderate orthoses, the compressive APS occurred at G4, G5 and G7, the middle of the neck and heel. The same for the Standard orthosis, the compressive APS at G3, G8, G4 and G5, all tested locations from lower-neck to heel were highly concentrated. The maximum compressive APS of the Flex orthosis is not at G2 anymore, but it shifted to G3 and G8, the lower-neck region and it was occurred on both sides. The magnitudes of the compressive APS of all types of orthoses had no significant difference. They are within the range from 0.45 MPa to 0.58 MPa.

Table 4.7 Magnitude and location of maximum peak stress for jumping

Orthosis Type	Magnitude & Location of Peak Stress	
	Tensile Peak Stress (0.1*MPa)	Compressive Peak Stress (0.1*MPa)
Varus	2.5 @ neck, lateral side	5.0 @ lower-neck, both sides & lower-neck, middle
Solid	6.3 @ upper-neck, both sides	5.5 @ neck, medial side & lower-neck, middle
Moderate	6.5 @ upper-neck, both sides	4.5 @ neck, medial side & lower-neck, middle
Standard	10.0 @ upper-neck, lateral side	5.1 @ lower-neck, both sides & lower-neck, middle
Flex	15.0 @ neck, lateral side	5.8 @ lower-neck, both sides

4.2.1.6 In Position Standing Up/Sitting Down: The tensile APS concentration was found primarily at G1 and G6 (Figure 4.16), the upper-neck on both sides with the Varus, the Solid and the Moderate orthoses. In addition, the tensile stresses in G4 were also noticeably high. For the Standard orthosis, it occurred at G1 and G2, the lateral side. For the Flex orthoses, it was located at G2 and G3.

The compressive APS was concentrated at G3 (lateral side arc region) with the Varus orthosis (Figure 4.17) However, it was almost even distributed in the neck and upper-neck region for the Solid, the Moderated and the Standard orthoses. The compressive APS at G2 and G6 for the Flex orthosis clearly showed a shear failure.

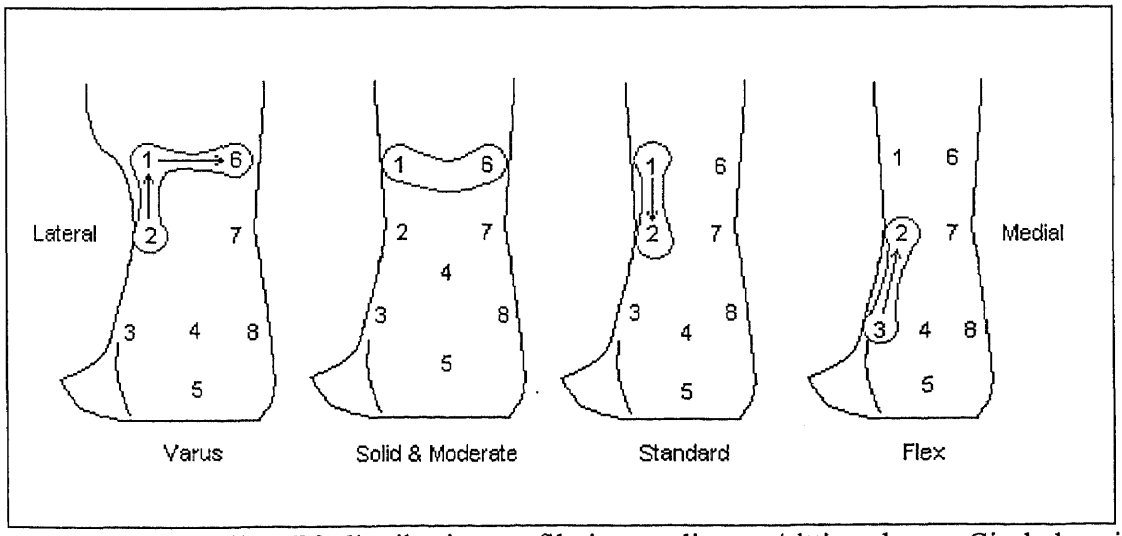

Figure 4.16 Tensile APS distribution profile in standing up/sitting down. Circled region shows the high APS concentration. Arrow indicates the change of the magnitude of APS from high to low. If no arrow indication, stresses are similar.

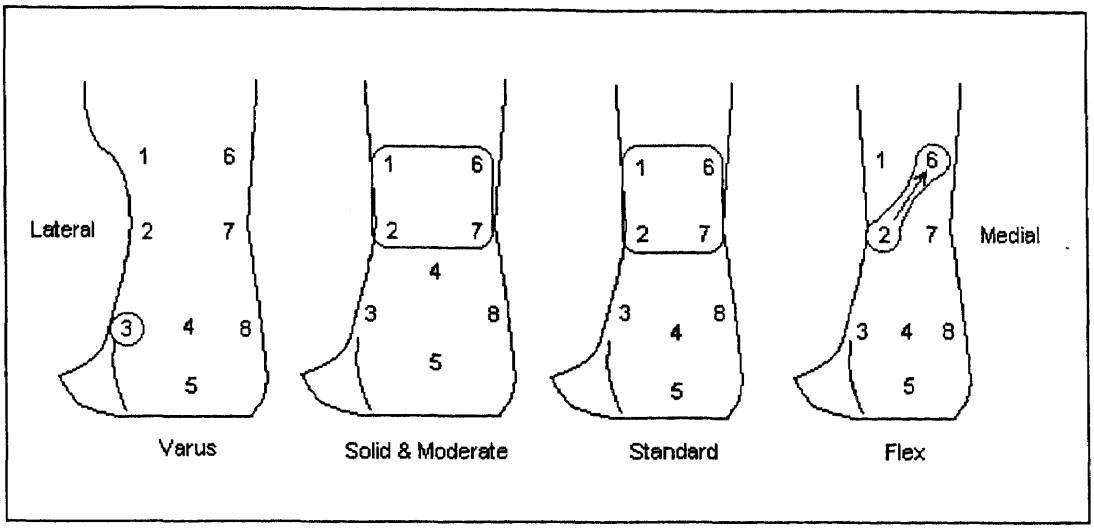

Figure 4.17 Compressive APS distribution profile in standing up/sitting down. Circled region shows the high APS concentration. Arrow indicates the change of the magnitude of APS from high to low. If no arrow indication, stresses are similar.

Table 4.8 Magnitude and location of maximum peak stress for standing up/sitting down

Orthosis Type	Magnitude & Location of Peak Stress	
	Tensile Peak Stress (0.1*MPa)	Compressive Peak Stress (0.1*MPa)
Varus	7.0 @ upper-neck, both side	5.7 @ arc edge, lateral side
Solid	8.0 @ upper-neck, both sides	6.3 @ neck & upper-neck, both sides
Moderate	8.4 @ upper-neck, both sides	3.5 @ neck & upper-neck, both sides
Standard	5.0 @ neck & upper-neck, lateral side	8.0 @ neck & upper-neck, both sides
Flex	6.2 @ neck & lower-neck, lateral side	5.5 @ neck, lateral side

4.2.1.7 In Position Lifting (25 lb. Object): Lifting (25 lb. object) had the same effect on the Varus, the Solid and the Moderate orthoses: the tensile APS was concentrated at

upper-neck region (Figure 4.18); the magnitudes were almost the same (0.2 MPa). For the Standard orthosis, the tensile APS, which was located at G1 and G2 (0.4 MPa), increased by 100%. With the Flex orthosis, it (0.75 MPa) was increased by 275% compared with that of the first three orthoses.

The compressive APS was found at different regions. For the Varus, it was located at G1 and G8 (Figure 4.19). For the Solid and the Moderate orthoses, it was concentrated at G4 and G7. For the Standard orthosis, it was found at G1 and G7, and it was primarily around the neck region of both sides. For the Flex orthosis, it was located at G2 and G6.

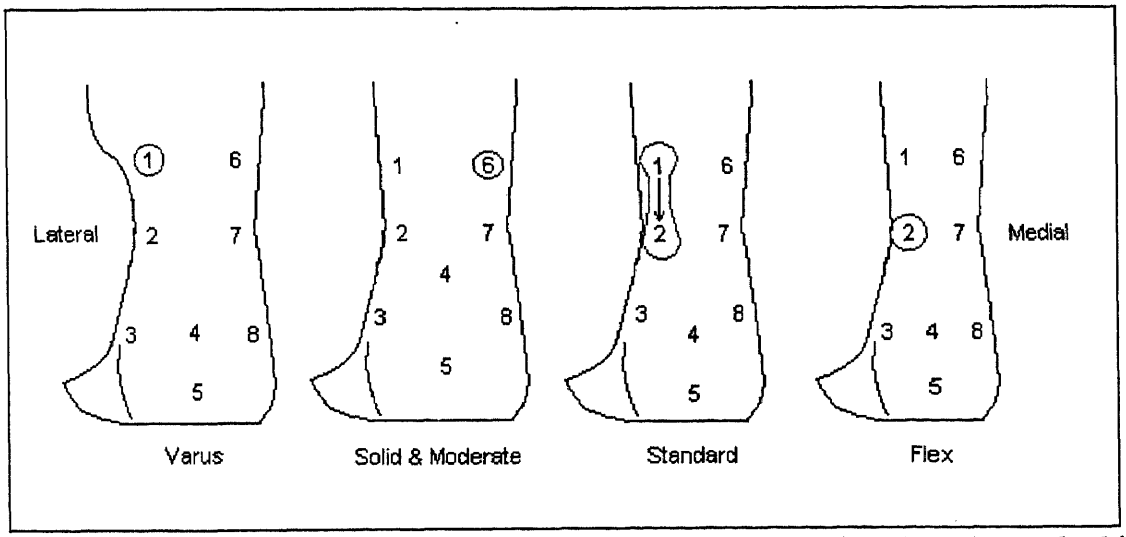

Figure 4.18 Tensile APS distribution profile in lifting. Circled region shows the high APS concentration. Arrow indicates the change of the magnitude of APS from high to low. If no arrow indication, stresses are similar.

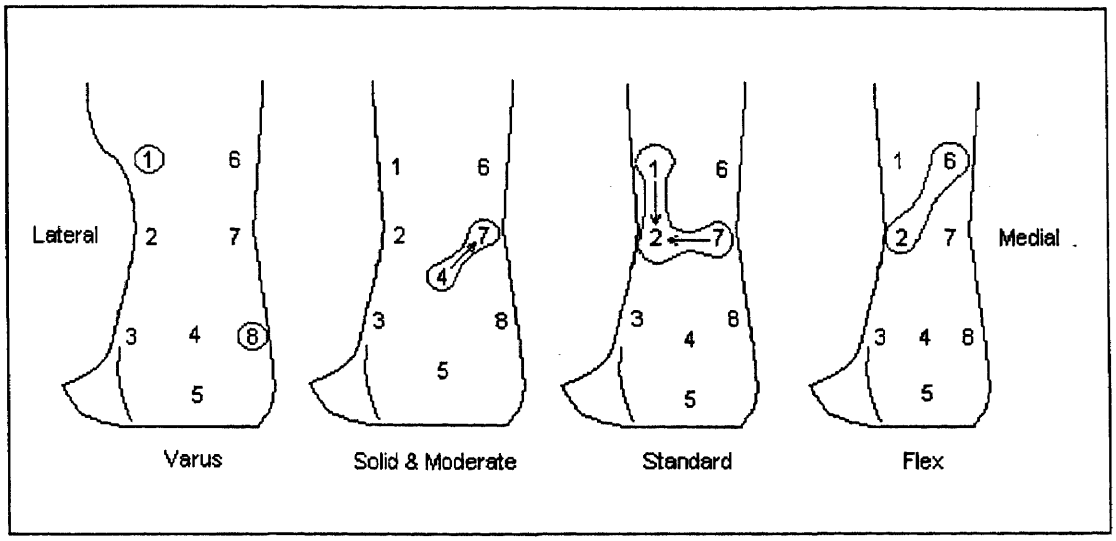

Figure 4.19 Compressive APS distribution profile in lifting. Circled region shows the high APS concentration. Arrow indicates the change of the magnitude of APS from high to low. If no arrow indication, stresses are similar.

Table 4.9 Magnitude and location of maximum peak stress for lifting

Orthosis Type	Magnitude & Location of Peak Stress	
	Tensile Peak Stress (0.1*MPa)	Compressive Peak Stress (0.1*MPa)
Varus	1.8 @ upper-neck, lateral side	1.0 @ arc edge, medial side
Solid	2.0 @ upper-neck, medial side	3.1 @ neck, medial side & lower-neck, in the middle
Moderate	2.0 @ upper-neck, medial side	2.0 @ neck, medial side & lower-neck, in the middle
Standard	4.0 @ neck & upper-neck, lateral side	3.7 @ neck & upper-neck, both sides
Flex	7.5 @ neck, lateral side	4.0 @ neck, lateral side & upper-neck, medial side.

4.2.2 Motions Involved in the Swing Phase of a Gait

Three coupled movements were tested in the swing phase: Dorsiflexion/ Planterflexion (motions of the ankle joint), Inversion/Eversion (motions of the subtalar joint), and Abduction/Adduction (combined motions of ankle & subtalar joint).

4.2.2.1 Dorsiflexion/Planterflexion: The tensile APS (during dorsiflexion) and compressive APS (planterflexion) were all concentrated at the same place within each orthosis. They were located at G2 with the Varus, G1 and G6 for the Solid and Moderate orthoses, G1 and G2 for the Standard and the Flex orthoses (Figure 4.20 and Figure 4.21).

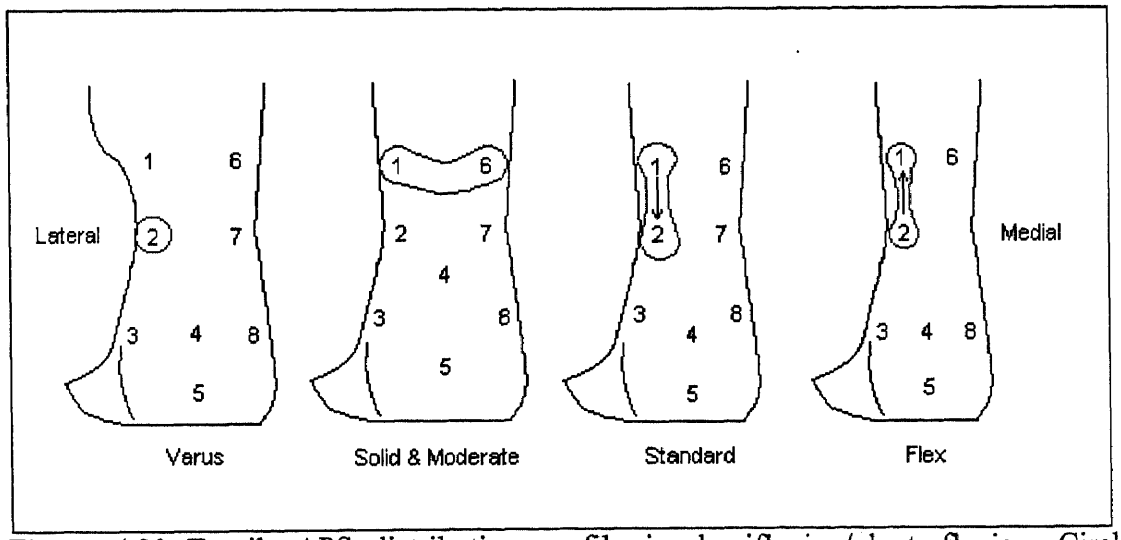

Figure 4.20 Tensile APS distribution profile in dorsiflexion/planterflexion. Circled region shows the high APS concentration. Arrow indicates the change of the magnitude of APS from high to low. If no arrow indication, stresses are similar.

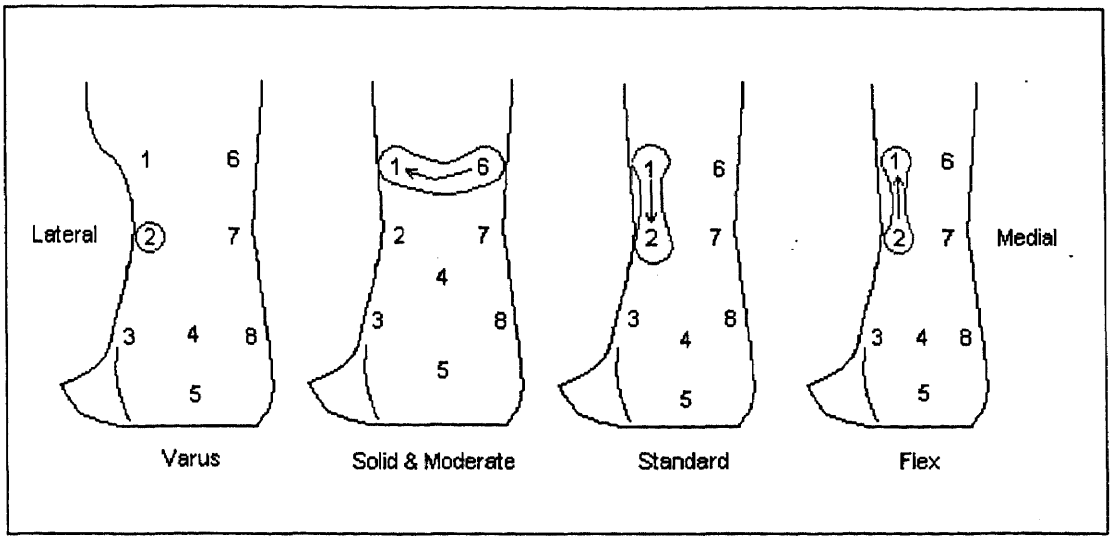

Figure 4.21 Compressive APS distribution profile in dorsiflexion/planterflexion. Circled region shows the high APS concentration. Arrow indicates the change of the magnitude of APS from high to low. If no arrow indication, stresses are similar.

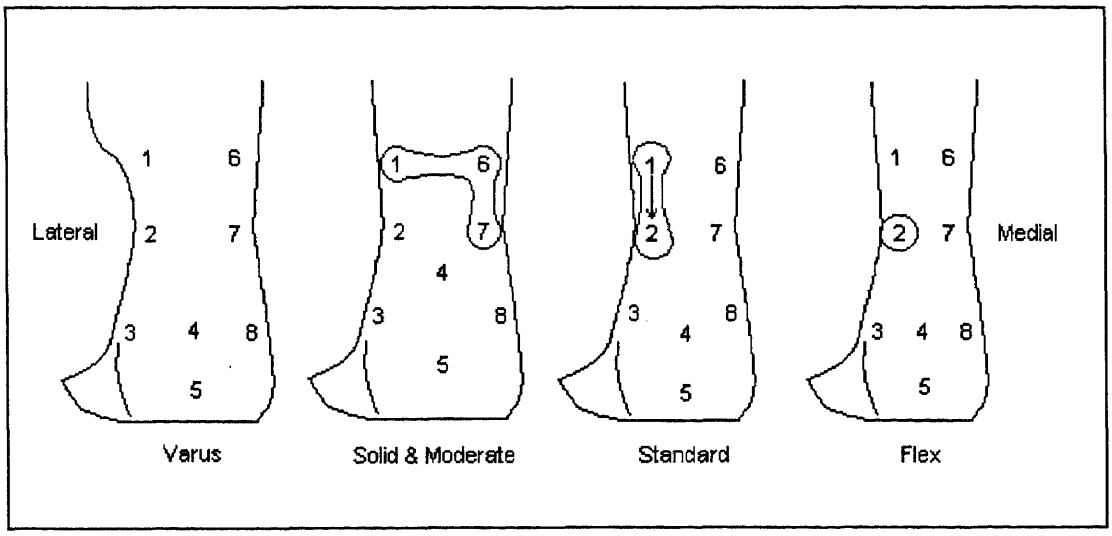

Figure 4.22 Tensile APS distribution profile in inversion/eversion. Circled region shows the high APS concentration. Arrow indicates the change of the magnitude of APS from high to low. If no arrow indication, stresses are similar.

4.2.2.2 Inversion/Eversion: All eight gages on the Varus orthosis indicated that the tensile stresses were not higher than 0.1 MPa. Therefore, no significant peak stress was determined. However, inversion/eversion did generate significant tensile peak stresses at

G6 & G7 for the Solid and the Moderate orthoses, as well as at G1 & G2 for the Standard orthosis, and G2 for the Flex orthosis (Figure 4.22).

4.2.2.3 Abduction/Adduction: Abduction/Adduction produced a distinct tensile APS distribution contour in every orthosis except for the Varus orthosis. The maximum tensile stress for the Varus AFO only occurred at G2, the neck of lateral side. For the rest of orthoses, the tensile APS occurred at G3 (the lateral side arc edge) and G6 (the medial side upper-neck edge) (Figure 4.23). In addition the compressive stress in the horizontal direction occurred at G3, arc edge of the lateral side. This compressive APS increased significantly during the abduction/adduction motion and it became the highest over all. Thus, abduction/adduction movement had a major effect on the side arc edge of the lateral side of the AFOs.

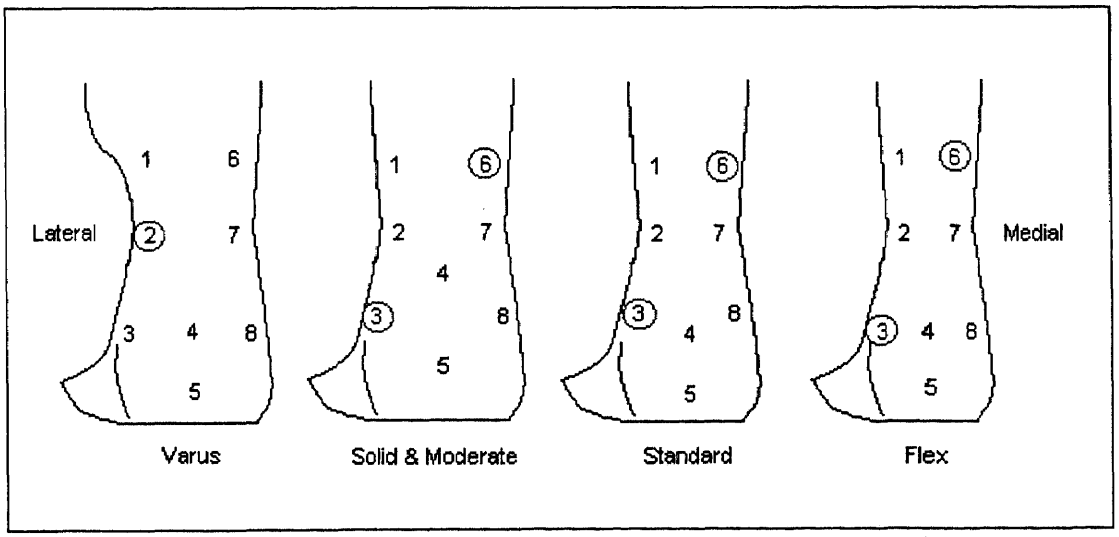

Figure 4.23 Tensile APS distribution profile in abduction/adduction. Circled region shows the high APS concentration. Arrow indicates the change of the magnitude of APS from high to low. If no arrow indication, stresses are similar.

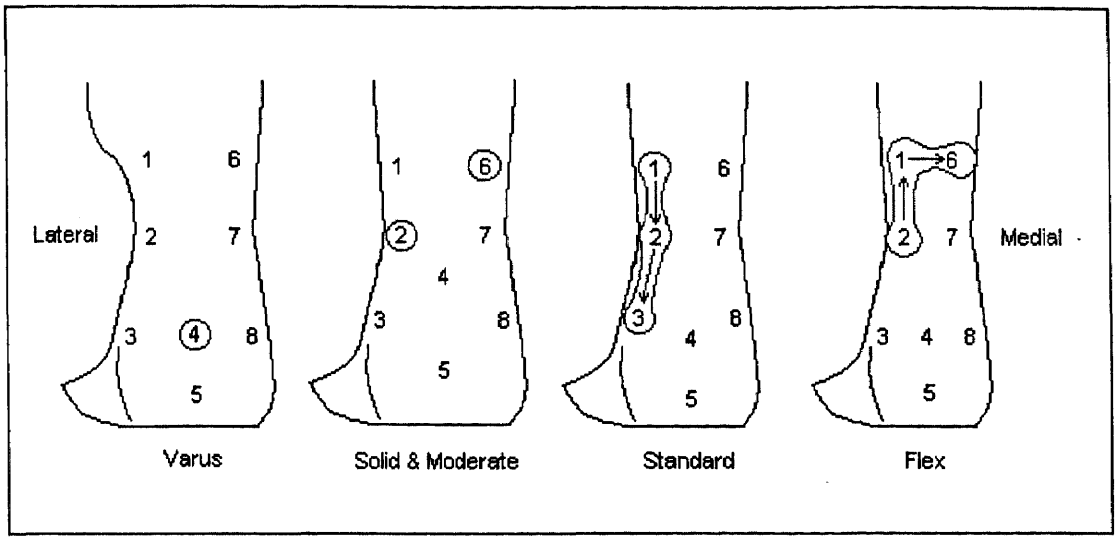

Figure 4.24 Compressive APS distribution profile in abduction/adduction. Circled region shows the high APS concentration. Arrow indicates the change of the magnitude of APS from high to low. If no arrow indication, stresses are similar.

CHAPTER 5

DISCUSSION

5.1 Motions Involved in the Stance Phase of a Gait

The magnitude and the location of the stress concentration determined from this experiment clearly indicated that the APS were dependent on the geometry (or the type) of the AFOs. In addition, they also depended on different patients and type of activities. A 200 lb. patient should generate a higher stress than a 100 lb. patient. However, this experiment will only concentrate on the study of stress change due to the change in orthosis geometries. Activities such as slow walk, fast walk, running and jumping all significantly altered the magnitude and location of the peak stress. Thus, the fatigue life or failure point of the orthosis can be predicted from the knowledge of the magnitude and location of peak stresses[12]. This confirmed our hypothesis stated earlier, and the FEA results.

5.1.1 Slow Forward Walk

Motion of slow walk forward is the most common human movement in nature. Slow walk usually occurred for the elderly, the disabled who needs some type of support, or a patient who is in or after the recovering process.

It was obvious that the tensile APS increased with an increasing in the flexibility of the orthosis. For the Flex orthosis, the tensile APS was located at G2, G6 and G3. It clearly showed a shear failure. This was observed during clinical study for the Flex

orthosis. It confirmed that this was the easiest point to break. The Compressive APS was concentrated at the upper-neck, and the tensile APS was concentrated at the neck. Results from the dynamic analysis of walk forward slowly clearly indicate that both tensile and compressive stress in the AFO were highly concentrated in the neck region. These peak stresses occurred during the heel strike (compressive) and toe-off (tensile).

From our observation, the ground contact point at the heel strike (beginning of the stance phase) is defined at the **lateral** bottom heel potion of the orthosis-shoe interface. When the heel strikes the ground, the maximum tensile APS in the orthosis was located at the **lateral edge** of the neck of the AFOs. The compressive peak stress (during the toe-off) in the orthosis was found to be at both sides of the neck region for symmetric AFOs, but only at the lateral side for asymmetric AFOs.

The results revealed that the peak stress concentration in the AFO varied significantly with a change of its types. However, each type of the orthosis has its own distinct stress distribution contour (Figure 4.5). For the Varus orthosis, it was concentrated at the neck of the lateral side. For the Solid and the Moderated orthoses, the stress was concentrated at the upper-neck area and on both sides. For the Standard orthosis, it was concentrated at the neck and upper-neck region of the lateral side. For the Flex orthosis, it was concentrated at the neck and lower-neck region of the lateral side. In general, the peak stress concentration was primarily located at the lateral side of the orthosis. The stress location shifted from the upper-neck to the lower-neck when the width of the neck reduced.

5.1.2 Fast Forward Walk

Motion of fast forward walk is a common human movement. Fast walk usually occurred for normal men and women who walks in the street/office for a short distance. Also patient who recovered from a strike but still need an AFO while doing normal daily activities, this motion is common.

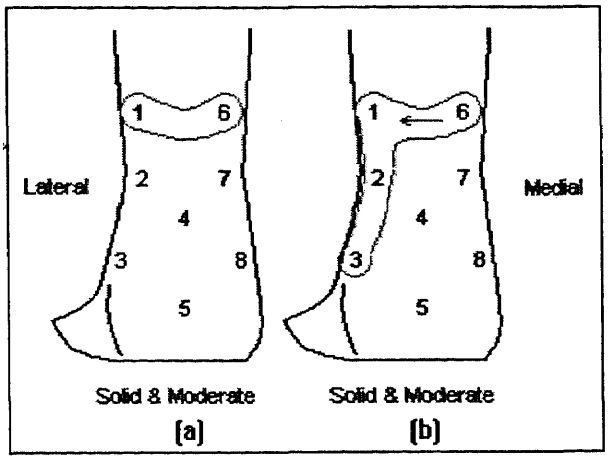

Figure 5.1 Comparison of the tensile peak stress distribution (toe-off) between slow walk and fast walk with the Solid and the Moderate orthoses. (a) slow forward walk; (b) fast forward walk. (Part of Figure 4.5 and Figure 4.7)

Results from the analysis of a fast forward walk revealed that both tensile and compressive stress in the asymmetric AFOs were highly concentrated in the neck region and they were located on the lateral side. Compared with the slow forward walk, except the increment of the magnitude of all stresses, fast walk did not significantly affect the stress distribution in the Varus and the Flex orthoses (Figure 4.6 & Figure 4.8). However, it did significantly affect the other three type of orthoses by shifting the peak stress concentration from both sides toward the lateral side and from the neck to the lower-neck region. This was due to the possibility of shifting the ground contact point. In addition,

this was also due to an increasing in walking velocity. Thus, loading forces were increased.

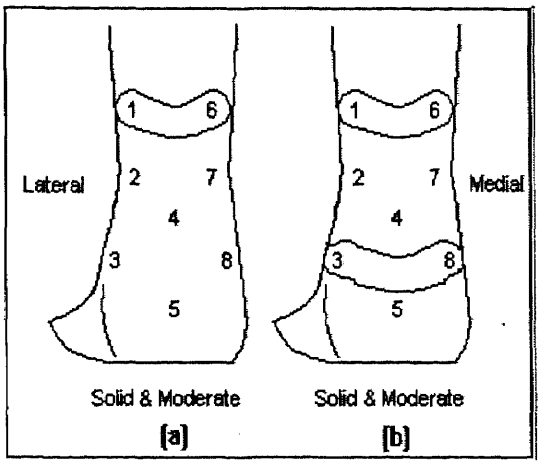

Figure 5.2 Comparison of the compressive peak stress distribution (heel strike) between slow walk and fast walk with the Solid and the Moderate orthoses. (a) slow forward walk; (b) fast forward walk. (Part of Figure 4.6 and Figure 4.8)

Again, compared with the slow forward walk, fast walk shifted the tensile stress concentration as well. It moved to the lateral side (Figure 5.1). The compressive stress concentration moved toward to the lower portion of the neck (Figure 5.2). This indicated that for a symmetric orthosis, it could have an asymmetric stress distribution.

5.1.3 Running

Running is defined as a movement faster than walk or a combined movement of forward walk and in-position jumping. Thus, there is a period when both feet will not contact the ground during running. For a more active movement, running should produce a different peak stress contour compared with those in fast walk. However, the results showed little

difference in APS distribution between fast walk and running. This was due to several factors in experiment:

- For the laboratory environment, there is not enough space for long distance running.
- The AFOs were connected to the fixed circuit board with a two-meter length cable which also limited the running distance.
- Wearing the orthosis made the subjects unable to run normally.
- The running velocity did not increase much compared with the fast forward walk.

The Varus orthosis showed that all APS were almost evenly distributed and all too small to be considered as the concentration point. Except for the lowest stress which occurred in G7, the neck of medial side (Figure 5.3).

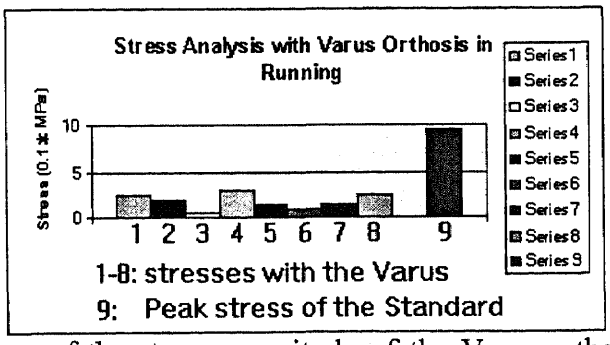

Figure 5.3 Comparison of the stress magnitude of the Varus orthosis and the Standard orthosis during running. 1-8: stresses from the strain gages on the Varus orthosis in the sequence of G6, G1, G7, G2, G8, G3, G4, G5. 9: APS of the Standard orthosis.

The Standard and the Flex orthoses had the same APS distribution as in fast walk. Only for the Solid and the Moderate orthoses, there were some differences. For example, the secondary concentration in lower-neck of both lateral and medial sides in fast walk disappeared. Instead, G4 and G5 (Figure 5.4), the middle of the lower-back of the

orthosis turned out to be the second highest tensile stress concentration. It demonstrated that besides some features of fast walk, running has intensive effects on the middle of the neck of the orthosis during heel strike.

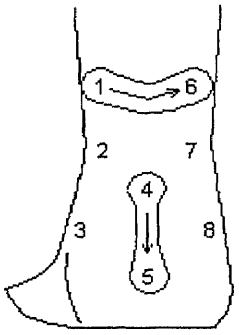

Solid and Moderate

Figure 5.4 Tensile APS distribution during running with the Solid and Moderated AFOs. (Part of Figure 4.9)

5.1.4 Backward Walk

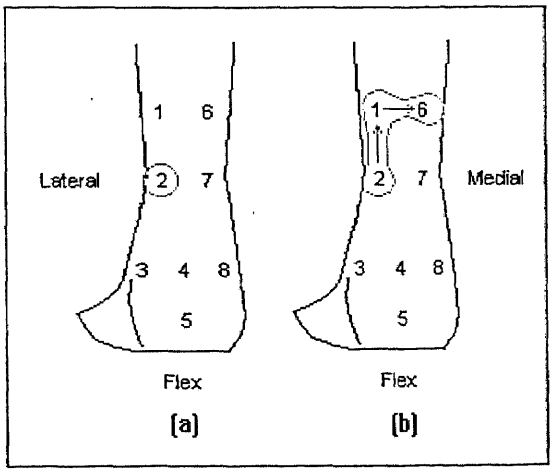

Figure 5.5 Comparison of the compressive peak stress concentration distribution with the Flex orthosis. (a) forward walk; (b) backward walk. (Part of Figure 4.6 and Figure 4.13)

Although backward walk is not as common as forward walk, it is part of daily activities. It usually occurred before sitting down, while vacuuming the carpet, or cleaning the floor with a mop. Therefore, it is necessary to be simulated and tested.

Since backward walk is the reverse movement of forward walk, the APS concentration is almost the same as that of slow forward walk. However, there is one clear difference between these two movements. The peak stress shifted from the neck (during slow forward walk) to the upper-neck. Especially for the Flex orthosis, the compressive stress concentration shifted from G2 (during slow forward walk) to G2, G1 and G6 region during backward walk (Figure 5.5).

5.1.5 In Position Jumping (Approximately 4 inches high)

Although jumping is not a common motion for patients who just suffer a stroke, it is common for people who is recovered after 2 to 3 years and still need wear an AFO. It was observed that a shear failure of the AFO would occur after jumping for several times. Thus, jumping has a significant effect on the orthosis failure and a simulation of this movement is necessary.

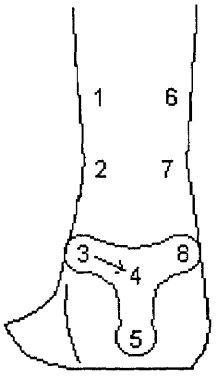

Figure 5.6 An example of compressive APS distribution in jumping. (part of Figure 4.15)

Except for the increment of the stress magnitude, there is no significant difference in tensile stress distribution in AFO compared with those in walking. However, the results of the compressive stress distribution from all five orthoses demonstrated that jumping had a significant effect on AFO. The compressive peak stress shifted from the neck (in slow walk) to the lower-neck and heel region of all orthoses in jumping (Figure 5.6).

5.1.6 In Position Standing Up/Sitting Down

Standing up/sitting down is a common daily activity for everybody. It is the earliest and yet the hardest motion for the patients to balance their body. Thus, in order to improve the design of AFO for better support, this is one of the most important movements that needs to be tested.

Results revealed that there is no obvious difference in the stress distribution between orthoses in standing up/sitting down. Unlike walk, jumping or other motions, the neck of the orthosis was not significantly influenced by this movement. However, the magnitude of the tensile peak stress in the Varus (0.7 MPa), the Solid (0.8 MPa) and the Moderate (0.84 MPa) orthoses were higher than those of the Standard (0.5 MPa) and the Flex orthoses (0.62 MPa). This was due to the fact that the patient exerted more force on the wider-necked orthosis in order to stand up. Moreover, the magnitude of the peak stress also depends on how fast the person stands up/sits down; that is, the faster the motion of standing up or sitting down, the more the stresses change. This indicated that the wider-necked orthosis should be prescribed to slow recovering patients or those

patients in the earliest stage of recovery. The wider the neck, the easier for the patients to balance themselves.

5.1.7 In Position Lifting (25 lb. Object)

Lifting objects is a normal part of daily activity. Most patients who lift small objects do not significantly change the stress distribution. However, for those recovered patients who still need an AFO and need to lift heavy objects, the stress distribution will be altered.

Lifting (approximately 25 lb.) object had the same effect on the Varus, the Solid and the Moderate orthoses. The tensile APS was concentrated at the upper-neck region. The magnitudes were almost the same (0.2 MPa). For the Standard orthosis, the tensile APS, which was located at G1 and G2 (0.4 MPa), increased by 100%. For the Flex orthosis, the tensile peak stress (0.75 MPa) was increased by 275% compared with the first three orthoses (Table 4.9). While the flexibility of the orthosis was enhanced, the tensile peak stress increased sharply. Results revealed that lifting had minor effect on the Varus, the Solid and the Moderate orthoses. However, it had a profound effect on the Flex and the Standard orthoses. This indicated that wider-necked orthoses should be prescribed to the worker who is doing lifting jobs.

5.2 Motions Involved in the Swing Phase of a Gait

5.2.1 Dorsiflexion / Planterflexion

Dorsiflexion/planterflexion is the motion at the ankle joint. It is the most important motion in the swing phase. During this motion, the flexibility versus stability of different type of AFOs[10] can be observed. It is also the common daily activity for people who need to drive, for example, taxi drivers.

The tensile and compressive APS profiles of dorsiflexion/planterflexion (during different period) were almost the same as during slow walk for most of the AFOs. However, they clearly pointed out that the maximum peak stress magnitudes of different orthoses rely on the width of their necks (Figure 5.7). The magnitude of compressive stress (at the neck region) increased when the width of the AFO's neck decreased. This phenomena can be interpreted as: a decrease in stress sustain area would result in a increase in stress concentration[2]. Although the width of the Varus and the Solid orthoses were the same at neck region, the support part on the lateral side of the Varus orthosis influenced dorsiflexion/planterflexion. Therefore, except for the Varus orthosis, these two parameters (width of the neck and the compressive APS) have a linear relationship. These two lines (as indicated in Figure 5.7) have the same slope. It suggested that the magnitude of compressive peak stress during dorsiflexion/planterflexion was able to be estimated from the width of the AFO's neck. Thus, the material failure due to this motion can be predicted. The narrower the neck, the easier to fail. The narrow-necked orthosis is not suitable for a person who needs to drive a lot.

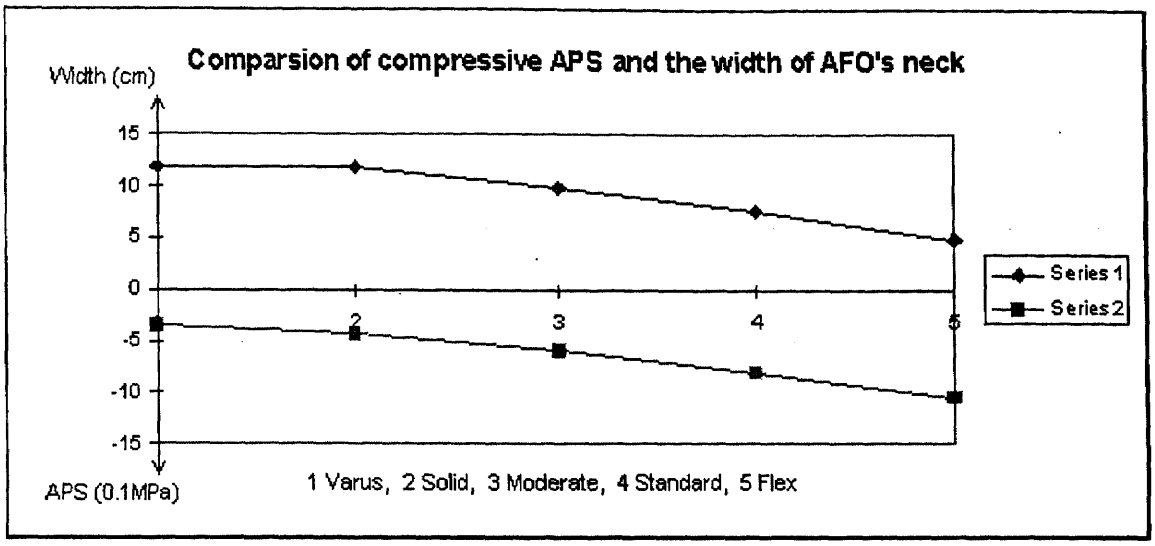

Figure 5.7 Comparison of compressive APS in dorsiflexion/planterflexion with the width of AFO's neck. Series 1 refers to the maximum compressive APS, series 2 refers to the width of the neck. point 1-5 in horizontal axis refer to Varus, Solid, Moderate, Standard and Flex orthoses.

5.2.2 Inversion/Eversion

Inversion/eversion is the motion at the subtalar joint. This motion occurred slightly in normal people. However, the patient who has a specity, an involuntary movement, presents excessive inversion/eversion.

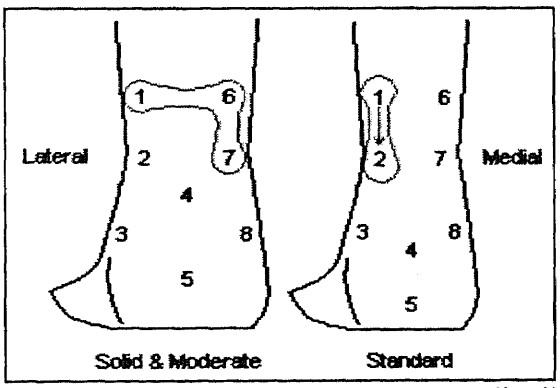

Figure 5.8 Comparison of the tensile peak stress distribution profile during inversion/eversion. (Part of Figure 4.20)

Inversion/eversion generated a tensile peak stresses in the neck (medial) region for the Solid and the Moderate orthoses, as well as in the neck (lateral) region for the Standard and the Flex orthoses. The tensile peak stress distribution profile (Figure 5.8) implied that the medial side of the Solid & the Moderate AFOs and the lateral side of the Standard & the Flex AFOs were more susceptible (easier to break) than the opposite side during inversion/eversion. However, the above movement had no significant influence on the Varus orthosis. All eight strain gages on the Varus orthosis indicated that the stresses were not higher than 0.1 MPa. On the other hand, the peak stress measured in the Solid orthosis was 0.55 MPa. It demonstrated that the inversion/eversion was prohibited by the additional support material added to the lateral side of the Varus AFO.

5.2.3 Abduction/Adduction

Abduction/Adduction is the combined motions of ankle and subtalar joints. Abnormal heel strike is due to toe drag and foot abduction.

Abduction and adduction produced a distinct tensile APS distribution contour in all tested orthoses except the Varus one. The maximum tensile stress for the Varus AFO was at the neck of the lateral side. For the rest of orthoses, the tensile APS was located at the lateral side arc edge and the medial side upper-neck edge (Figure 4.21). The compressive APS at the lateral side arc edge was noticeably increased and became the highest of all. Thus, abduction/adduction had major effect on the lateral side arc edge of the orthoses. The AFO that is prescribed for people who suffer the toe drag with abduction should have reinforcement at the lateral side arc edge.

5.3 Summary

Parametric analysis revealed that the geometry of orthosis plays an important role in the determination of peak stress distribution. For some motions, such as running and jumping, the tensile peak stresses in the neck region on the lateral side of the Flex orthosis were above the material yield strength (Figure 5.9), which means that plastic deformation occurred and it produced an unrecoverable strain. After the experiment, the lateral side of the Flex orthosis discolored. Thus, the material was already fatigued. The original capacity of the material to sustain stress was no longer existed. There was no tensile peak stresses exceeding the yield strength on other AFOs. On the other hand, there was no compressive peak stress exceeding the yield compressive strength (Figure 5.10), although some of them were very close to it. There are two primary factors that cause material to fail are: high-stress with low-cycle failure and low-stress with high-cycle failure. The former failure happened with the Flex orthosis and the latter happened with other orthoses, especially the Varus orthosis. Figure 5.9 and Figure 5.10 indicated the magnitude of peak stress from high to low in the AFOs due to movements was in the sequence from the Flex, Standard, Moderate, Solid to Varus. It further confirmed that the more flexible, the less stable and the higher the stress.

During the swing phase, the peak stress of different types of orthoses rely on the width of the neck during dorsiflexion/planterflexion and they had a linear relationship. Thus, the peak stress in dorsiflexion/planterflexion can be predicted from the width of the AFO's neck. The material failure due to this motions can be predicted. The narrower the neck, the easier to failure. The inversion/eversion generated tensile peak stresses in the

neck (medial) region of the Solid and the Moderate AFOs, as well as in the neck (lateral) region of the Standard and the Flex orthoses. The medial side of the Solid and the Moderate orthoses and the lateral side of the Standard & the Flex AFOs were more susceptible (easier to break) than the opposite side during inversion/eversion. Abduction/adduction produced a distinct tensile APS distribution contour. The peak stress concentration was found at the arc edge of the lateral side and the upper-neck edge of the medial side.

Second sample with an approximately 145 lb. loading force was tested after the first one (170 lb.). Although the magnitude of the APS was not the same, the stress distribution almost identical for the five AFOs. There was only a minor difference between these two samples. The effect on AFOs due to loading will be studied at the next experiments.

Based on the data analysis, we suggested to the orthotist should consider not prescribing the Flex orthosis to children or active people who are involved in outdoors activities such as jumping and running. Instead, using the asymmetric Standard orthosis that is a little bit wider in the lateral side which would provide the same flexibility and lower peak stress. In fact, we suggest every orthosis should be made asymmetrically. However, the AFO should have a wider lateral side than the medial side. The Flex orthosis could be used for a more active people if the lateral side neck region of the Flex orthosis is strengthened. On the other hand, the Flex orthosis is recommended to be used by drivers whose general activities would be dorsiflexion/planterflexion (stepping on the

gas or brake). The Flex orthosis was more comfortable, convenient and increased only 7% compressive stress than the Standard orthosis in dorsiflexion/planterflexion.

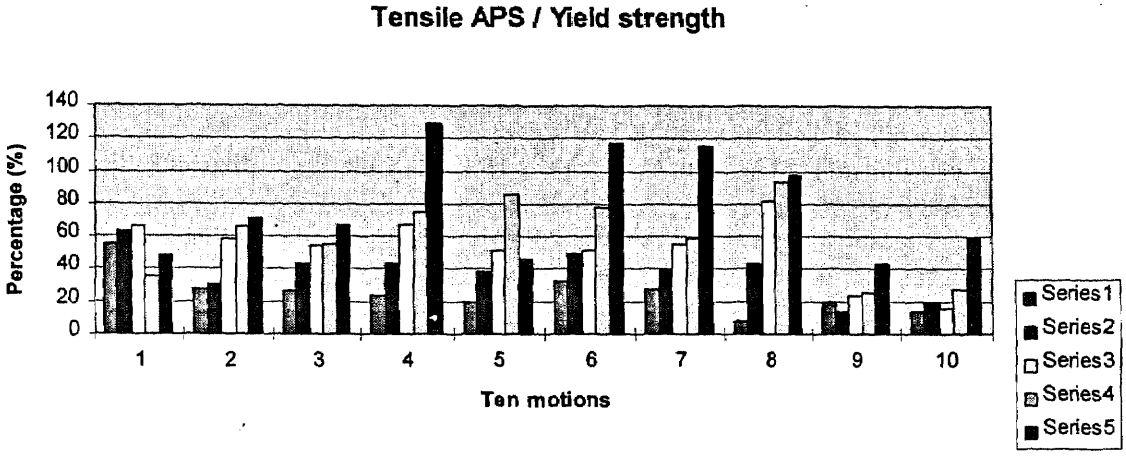

Figure 5.9 Percentages of the tensile peak stress/yield strength in ten motions. 100% in vertical axis indicates the tensile yield strength (σ_Y).
Five (orthosis) series are: 1. Varus, 2. Solid, 3. Moderate, 4. Standard, 5. Flex.
Ten motions are: 1. stand up/sit down, 2. slow forward walk, 3. fast forward walk, 4. running, 5. slow backward walk, 6. jumping, 7. dorsiflexion/planterflexion, 8. inversion/eversion, 9. abduction/adduction, 10. lifting (25 lbs. object).

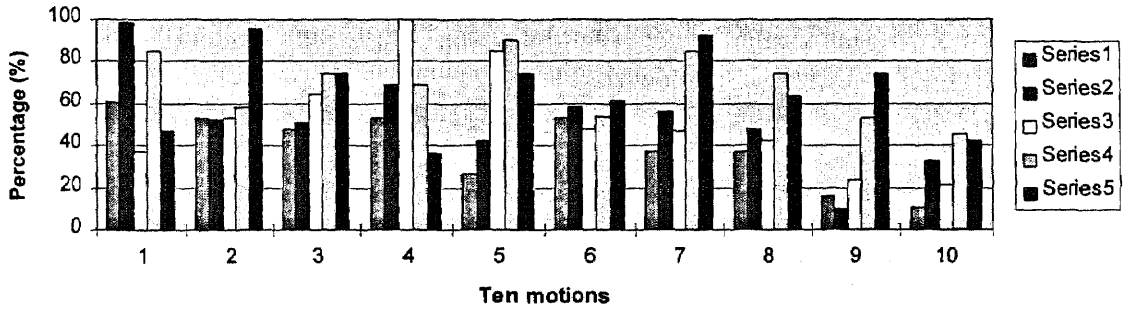

Figure 5.10 Percentages of the compressive peak stress/compressive yield stress in ten motions. 100% in vertical axis indicates the compressive yield strength (σ_Y).
Five (orthosis) series are: 1. Varus, 2. Solid, 3. Moderate, 4. Standard, 5. Flex.
Ten motions are 1. stand up/sit down, 2. slow forward walk, 3. fast forward walk, 4. running, 5. slow backward walk, 6. jumping, 7. dorsiflexion/planterflexion, 8. inversion/eversion, 9. abduction/adduction, 10. lifting (25 lbs. Object).

CHAPTER 6

CONCLUSION AND RECOMMENDATION

6.1 Summary

We have successfully accomplished the objectives of this investigation. That is, we have developed a complete experimental procedure to collect and analyze data. We have conducted an extensive parameter analysis for the prediction of AFO failure. We have developed instrumentation that could be used to record the strains at various locations simultaneously.

Overall analytical results from the dynamic analysis clearly indicate that both tensile and compressive stresses in all type of AFOs were highly concentrated in the neck region. During the regular activities, the maximum tensile and compressive stresses for the Varus orthosis were all small, and approximately evenly distributed. For the Solid and the Moderate orthoses, the maximum stresses always occurred at the upper-neck of both side. For the Standard orthosis, it was found that both tensile and compressive stresses (during different periods) occurred at the neck and upper-neck region on the lateral side. For the Flex orthosis, it was concentrated across the neck. It clearly shows a shear failure, the same as most failed Flex orthosis in clinical observations. For both the Standard and the Flex orthoses, their peak stresses were highly concentrated in the neck region of the lateral side. It confirmed the former FEA[1, 4] results that this was the easiest point to fail.

The present experimental results are consistent with earlier 3-D FEA results. Also, the results confirmed that the maximum peak stress occurs in the neighborhood of the

neck region of the AFOs and the stress distributions are asymmetric. In addition, it is worthy to measure the second sample (applied approximately 145 lb. loading force) after the first one (170 lb.). The results were similar to those from the first sample.

Note that the second hypothesis in the FEA analysis could not be confirmed. The hypothesis stated that during the stance phase, a high stress was produced in the heel region with the ground contact point located at the center of the heel of the orthosis-shoe interface. In the present experiment, it was difficult to install strain gage at the position and keep it there during motion.

6.2 Findings

The results revealed that the peak stress concentration in the orthoses varied significantly with a change of the orthosis type. However, each type of orthosis has its own distinct stress distribution contour. Specifically:

1. For the Varus orthosis, the peak stress (either tensile or compressive) was concentrated at the neck of the lateral side.
2. For the Solid and the Moderated orthoses, the peak stress was concentrated at the upper-neck area of both side.
3. For the Standard orthosis, it was located at the neck and the upper-neck region of the lateral side.
4. For the Flex orthosis, it was located at the neck and the lower-neck region of the lateral side.

The stress distribution was also altered by different type of motions. However, each motion had its distinct effects on the orthoses.

1. Compared with slow walk, fast walk made the peak stress concentration shift to the lateral side and the lower-neck region due to the shifting of ground contact point at the bottom flat potion of the AFO.
2. Running has intensive effects on the middle of the back of the orthosis during heel strike.
3. All five orthoses demonstrated that jumping had a significant effect on the lower-neck and heel region of the AFOs.
4. Form the overall peak stress magnitude, standing up/sitting down and lifting 25 lbs object had no significant difference between orthoses.

The stance phase of a normal individual consists of heel strike, foot flat, and toe-off. The dynamic analysis clearly indicated that heel strike and toe-off have the highest possibility to cause the orthosis to fail. The result revealed that the tensile stresses are highly concentrated in the neck region during these two periods. The results suggest that the orthosis would fail in the neck region, which is consistent with the FEA[1] results and the clinical observations[14].

During the swing phase, the peak stress of different types of orthoses rely on the width of the neck during dorsiflexion/planterflexion and they have a linear relationship. Thus, the peak stress in dorsiflexion/planterflexion can be predicted from the width of the AFO's neck. The material failure due to this motion can be predicted. The narrower the

neck, the easier to fail. The inversion/eversion generated tensile peak stresses in the neck (medial) region of the Solid and the Moderate AFOs, as well as in the neck (lateral) region of the Standard and the Flex orthoses. The medial side of the Solid & the Moderate orthoses and the lateral side of the Standard & the Flex AFOs were more susceptible (easier to break) than the opposite side during inversion/eversion. Abduction/adduction produced a distinct tensile APS distribution contour. The peak stress concentration was found at the arc edge of the lateral side and the upper-neck edge of the medial side.

Most stresses occurred at the neck region in vertical direction. Though the stress in horizontal direction (90°⊥) did play some roles in the overall failure, its magnitude in most cases was approximately half of that in the vertical direction.

6.3 Recommendation

The strain gage installation procedures in the present investigation were successfully applied[13]. However, failures of perfect bonding between the measuring surface and the strain gage still occurred at the solder tab. Preattached leadwires can eliminate the need for soldering to the gage or terminal altogether in many applications. With the proper strain gage accessories and installation techniques, lifted soldering tabs can be virtually eliminated.

Although an extensive peak stress analysis was finished, there are other factors that of the AFOs might be valuable to analyze in order to improve the design and manufacture process. For example: an energy consumption parameter could be used to

indicate the support ability of different AFOs. Like the peak stress, the amount of energy absorbed by the orthosis might cause its shear failure in certain regions.

In the present investigation, only five plastic AFOs were tested. There are many different AFOs currently being used. For example: a newly designed AFO, Generation II[15], (using stress-relieved polypropylene, free or locking poli-axial hinge) has many attractive features and performances for the patients. It has low profile, high strength, light weight, and easy application. Furthermore it can provide positive counter-rotatory action. Further study will reside at the experiment stress analysis and FEA for more type of AFOs.

APPENDIX

COMPARISON OF METAL AND PLASTIC AFO

	Metal AFO	Plastic AFO
Weight	Fairly heavy	Relatively light
Cost	Similar	Similar
Cosmetic appearance	Poor	Good
Patient's acceptance	Fair	Good
Proper and comfortable fit	Good	Excellent
Chances of producing damage to clothes	Potentially present	Usually absent
Choice of footwear	Limited	Unlimited
Plantar flexion and dorsiflexion of the ankle	can be free	Fairly limited
Proper fit on a swollen lower leg	Quite possible	Almost impossible
Mediolateral ankle stability	Good	Variable, depending on the orthotic types
Durability	Very good	Variable, depending on the orthotic types

REFERENCES

[1] T. Chu, N. P. Reddy and J. Padovan, "Three-dimensional finite element stress analysis of the polypropylene, ankle-foot orthosis: static analysis," *Med. Eng. Phys.* vol. 17, no.5, pp.372-379, 1995.

[2] K. K. Wu, *Foot Orthoses Principles and Clinical Applications*, Baltimore, MD: Williams & Wilking, 1990.

[3] W. Bunch and R. Keagy, *Principles of Orthotic Treatment,* St. Louis, MO: C.V. Mosby, 1976.

[4] T. Chu and Narender P. Reddy, Stress distribution in the ankle-foot orthosis used to correct pathological gait," *J. of Rehabil. Research and Development*, pp.349-360, vol. 32, no. 4, 1995.

[5] Jchiro Kawamura, Jiro Kawamura, M.D., "Some Biomechanical evaluations of the ISNY flexible above-knee system," *Orthotics and Proth.*, 40:20-22, 1986.

[6] P. Convery and J. Hughes, "A clinical evaluation of an ultralightweight polypropylene below-knee prosthesis," *Orthotics and Prosth.*, pp.30-37, vol. 40, no. 3, 1986.

[7] Joyce M. Howard and Agnes F. Holland, *Wilson Applied Science and Technology Abstracts*, Princeton, NJ: Princeton University Press, 1995.

[8] N. P. Reddy, G. Pohit, P. C. Lam, R. C. Grotz, "Finite element modeling of the ankle-foot orthoses," *Proc Inter Conf Biomechanics and Clinical Kinesiology of Hand and Foot,* Indian Inst. of Tech., 97-9, 1985.

[9] J. E. Tomaro and S. L. Butterfield, "Biomechanical treatment of traumatic foot and ankle injures with the use of foot orthotics," *J. of Orthop. Sports Phys. Ther.*, 21(6):373-80, 1995.

[10] Sumiko Yamamoto, Masahiko Ebina, Mitsuo Iwasaki, Shigeru Kubo, Hideo Kawai and Takeo Hayashi, "Comparative study of mechanical characteristics of plastic AFOs," *J. of Orthotics and Prosth.*, pp.59-64, vol. 5, no. 3, 1993.

[11] D. C. Kerrigan, M. A. Thirunarayan, L. R. Sheffler, T. A. Ribaudo and P. J. Corcoran, "A tool to assess biomechanical gait efficiency; a preliminary clinical study," *Am. J. of Phys. Med. Rehabil.*, 75(1):3-8, 1996.

[12] J. A. Collins, *Failure of Materials in Mechanical Design*, New York: John Wiley & Sons, 1981.

[13] T. Chu and A. Gent, "Bonding methods of strain gages to the polypropylene AFO," *Experimental Techniques*, vol. 20, no. 5, 1996.

[14] G. E. Doxey, "Clinical use and fabrication of the molded thermoplastic foot orthotic devices: suggestion from the field," *Physical Therapy* 65:1679-82, 1985.

[15] *American Journal of Physical Medicine and Rehabilitation*, vol. 74, no.1, Jan./Feb. 1995.